*ACE - European School of Antennas*

***"High-frequency techniques and travelling wave antennas"***

*Siena – Roma, February 21 – 26, 2005*

# The PO field evaluated by integration on the optical Shadow Boundaries

**ANTONIO PIPPI**

# SCATTERING BY LARGE OBJECTS

- Many typical applications of EM analysis require the evaluation of the scattering from large p.e.c. surfaces (RCS prediction, reflectors antennas, installation in complex platforms, etc.).

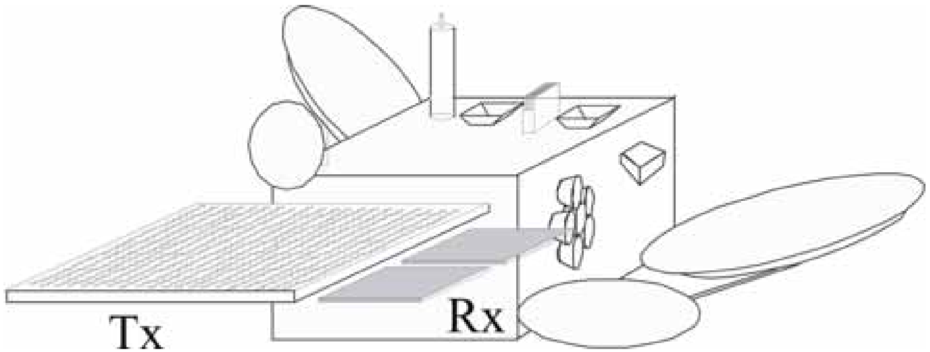


→ Electrically large and very large reflector antennas are used in several space applications, in both space and ground segments

→ Herschel-Plank (radio-telescope), 70m Ka-band DSN antenna
***$D \approx 5.000\ \lambda$***

- A suitable and not time-consuming solution to such scattering problems can only be given in the framework of high-frequency techniques

→ **design and verification activities**

# PHYSICAL OPTICS

- Physical Optics (PO) is the most widely used approach

→ versatile (unlike geometrical theories, does not require any specific canonical solution for each distinct geometric feature of the scatterer)

→ easy to be implemented (same scheme for all scatterers)

→ well-behaved in any observation region (no singularities or discontinuities in the field description, like caustics, SBs)

- In common implementations, the PO field is evaluated via the **2D** radiation integral over the surface currents

$$\boldsymbol{E}_s^{PO}(\boldsymbol{r}) = -j\frac{\varsigma}{k}\iint_{S_{lit}}\left\{\nabla\times\nabla\times\underbrace{\left(2\hat{n}\times\boldsymbol{H}_i(\boldsymbol{r}')\right)}_{\boldsymbol{J}^{PO}}\right\}\frac{e^{-jkR}}{4\pi R}\,dS'$$

- The computational cost is ***O(*$D_\lambda^2$*)***, where $D_\lambda$ is the size of the scatterer in terms of a wavelength

# PO FIELD OF LARGE OBJECTS

- When dealing with large bodies, PO requires the computation of double integrals with fast oscillating kernels (if ***kR » 1***)

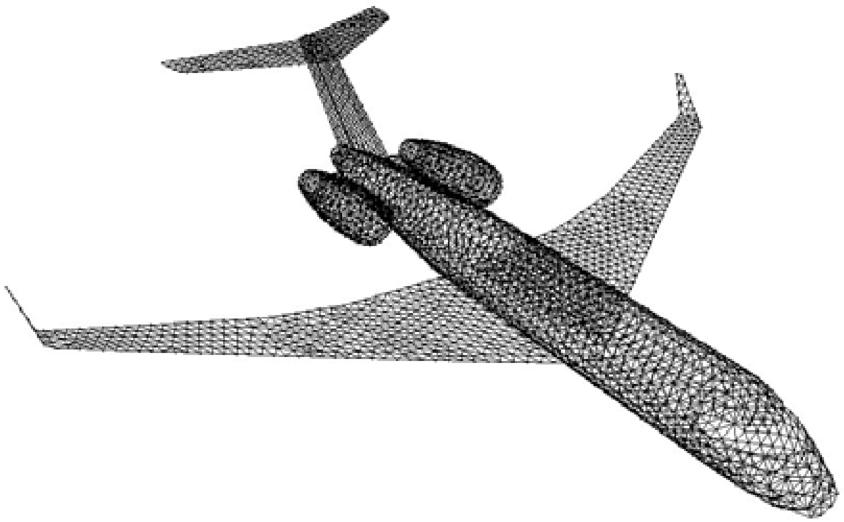

An aircraft modeled by flat triangular facets

(each facet is large in terms of $\lambda$ and small in terms of the local surface radius of curvature)

→ for applications of e.m. scattering by very large objects, the numerical integration is very time-consuming !!

very large reflectors
multiple bounce PO (multi-reflector systems, beam waveguides, etc.)

- Drastic reduction in requirements of CPU times and memory storage if the PO **surface integration** is reduced to a **line integration**

$$\boxed{O(D_\lambda^2) \longrightarrow O(D_\lambda)}$$

# SURFACE-TO-LINE REDUCTION OF PO INTEGRAL

$$\iint_S \boldsymbol{F}_{PO}(\boldsymbol{r};u,v)\,\mathrm{d}S \longrightarrow \oint_\ell \boldsymbol{f}_{PO}(\boldsymbol{r};\ell)\,\mathrm{d}\ell$$

- The representation is not unique

$$\oint_\ell \boldsymbol{f}_{PO}(\ell)\,\mathrm{d}\ell = \oint_\ell \{\boldsymbol{f}_{PO}(\ell) + \nabla\Phi(\ell)\}\mathrm{d}\ell$$

**irrotational field**

- Different formulations of the PO field from a flat metallic plate

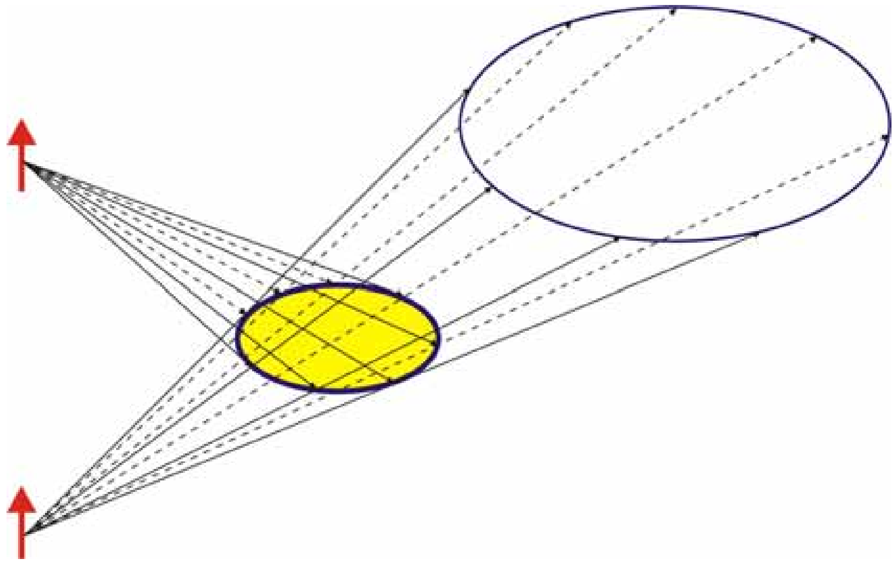

| | | |
|---|---|---|
| **M. Albani and S. Maci** | "An exact line integral representation of the PO radiation integral from a flat perfectly conducting surface illuminated by elementary electric or magnetic dipoles" | *Turk. J. Elec. Engin.*, vol. 10, n. 2, pp. 291-303, 2002 |
| **P. M. Johansen and O. Breinbjerg** | "An Exact Line Integral Representation of the Physical Optics Scattered Field: The Case of a Perfectly Conducting Polyhedral Structure Illuminated by Electric Hertzian Dipoles" | *IEEE Trans. Antennas Propagat.*, vol. AP-43, pp. 689-696, July 1995 |
| **K. Sakina and M. Ando** | "Line integral representation for diffracted fields in Physical Optics approximation based on field equivalence principle and Maggi-Rubinowicz transformation" | *IEICE Transaction on Communications*, Sep. 2001 |

# APERTURE RADIATION

- **Basic idea**

→ representation of the field radiated from a finite aperture in terms of **incremental contributions arising from its rim**

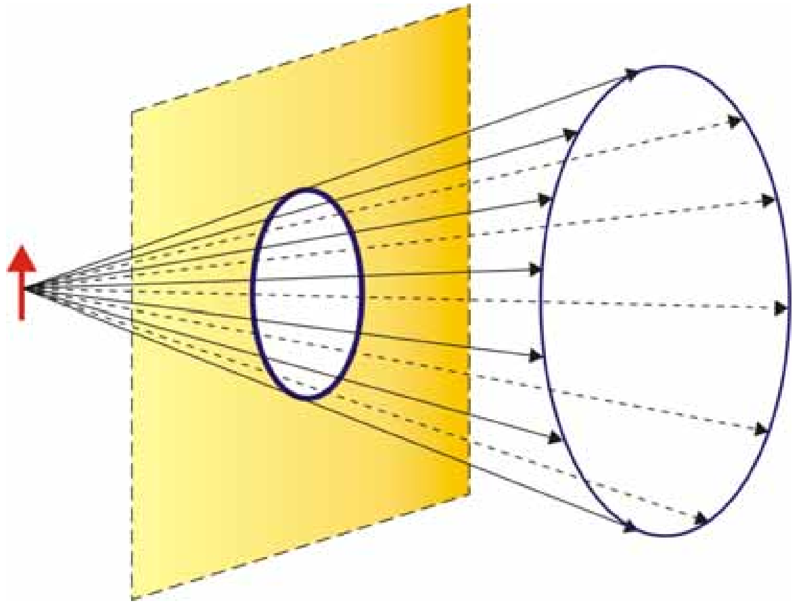

- Young (XIX Cent.)
- Maggi (1888), Rubinowicz (1917)

scalar optical-acoustical case

→ boundary waves as responsible of diffracted field

- **Surface-to-line reduction of Kirchhoff aperture radiation**
(derivation based on the Huygens' principle)

**A. Rubinowicz**, "Geometric Derivation of the Miyamoto-Wolf Formula for the Vector Potential Associated with a Solution of the Helmholtz Equation", *J. Opt.Soc. Am.*, vol. 52, n.6, pp. 717-718, June 1962

# PO FIELD OF A P.E.C. FLAT PLATE

Basing on Rubinowicz's philosophy (application of the equivalence principle) – **Albani, Maci, 2002**

- **projecting surface** from the observation point to infinity – passing through the plate's rim
- point-source illumination (electric or magnetic hertzian dipole → **PO GF**)

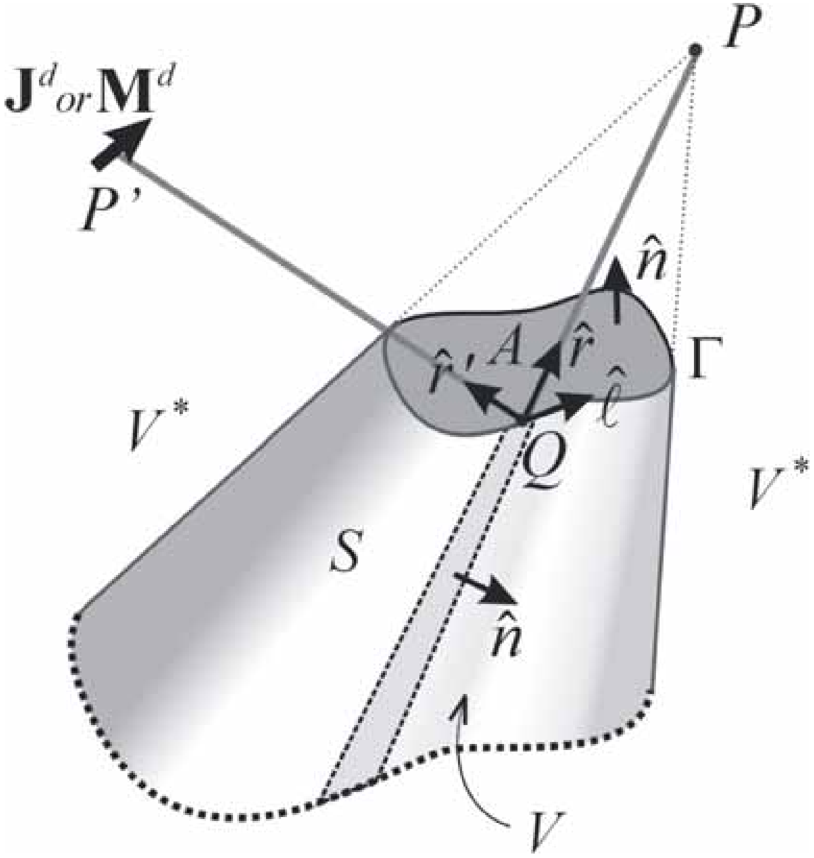


The plate is assumed in the far zone of the dipole

→ the **reactive** components of the incident field are **neglected** (→ simpler formulation)

→ the **spherical wave-front** assumption is preserved (plane wave incidence → restricting for **hybrid MoM-PO** applications)

→ **simpler, yet "exact"**, formulation for the incremental PO scattering coefficients.

- can be applied to the PO scattering from very large p.e.c. bodies described in terms of **facet segmentation**

# “CANONICAL” REFLECTORS

- **GO/AI field of a parabolic reflector**

**L. Infante and S. Maci**, “Near-Field Line-Integral Representation of the Kirchhoff-Type Aperture Radiation for a Parabolic Reflector”, *IEEE AWPL*, December 2003

→ feed with phase-center at the focus

→ the GO reflected field propagates along parallel rays

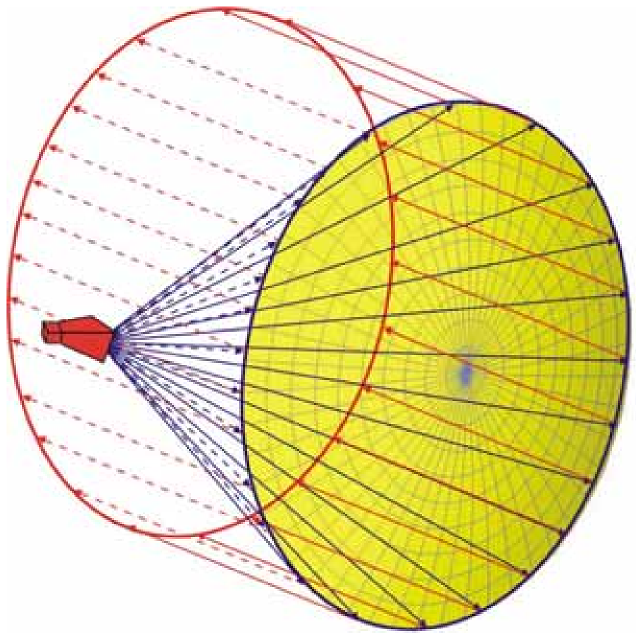

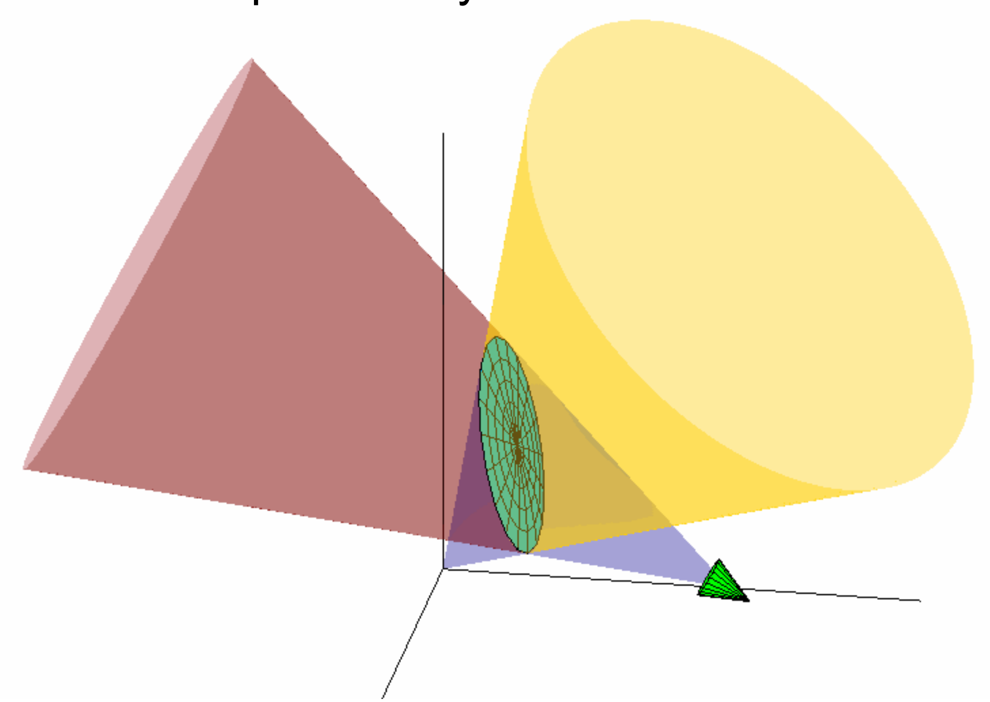

- **PO field of a hyperbolic reflector**

**A. Pippi, A. Caruso, M. Sabbadini and S. Maci**, “The Shadow Boundary Integral Technique for Cassegrain Subreflectors”, *IEEE AP-S Symp*, 2004

→ focal feed

→ image feed at the virtual focus

- All the distinct formulations can be cast (slight modifications…) in a unitary framework, the **Shadow Boundary Integral (SBI)** method

# SBI TREATMENT

- **1.** the PO field from the scattering surface is expressed in terms of a pair of integrals with domains on the Incidence and Reflection Shadow Boundary surfaces (**ISB** and **RSB**), truncated by the scatterer rim, plus the GO reflected field

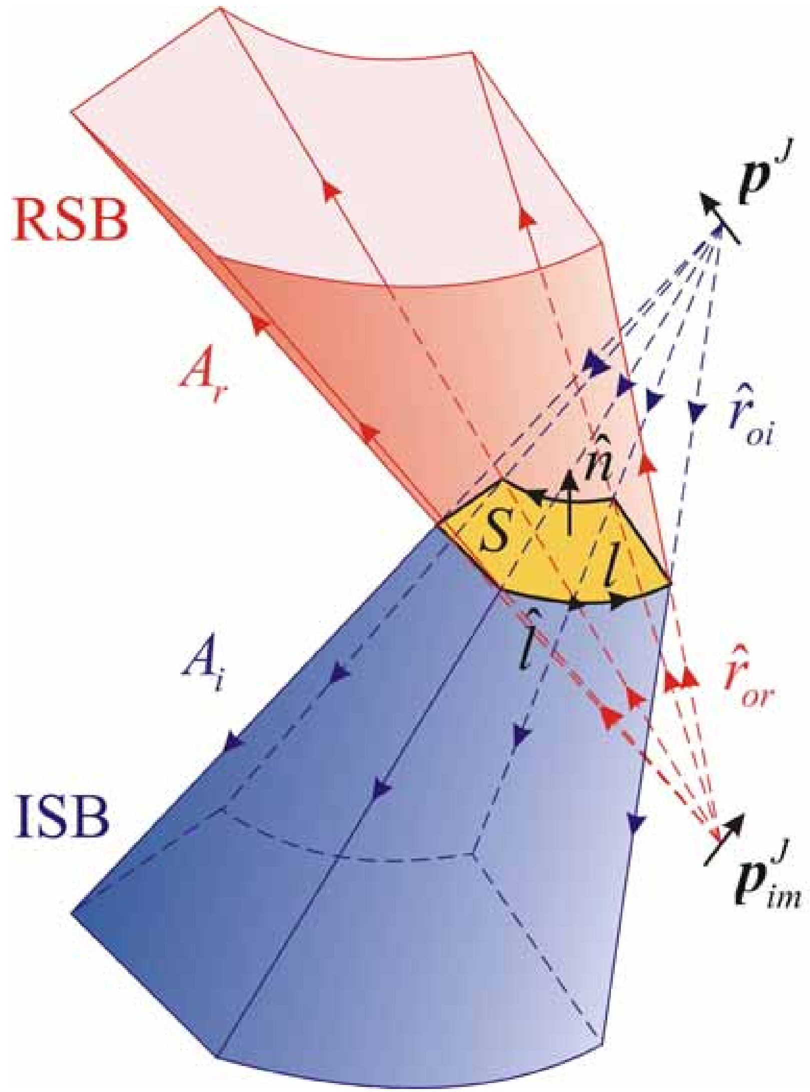


- **2.** the reduction of each of the two surface integrals to a line integral along the rim is obtained by **exact** closed-form evaluation along the Poynting vector direction (i.e., along the generatrices of the cone which projects to infinity the scatterer rim from the real or image source point)

→ **incident** and **reflected** ray-paths

# AUXILIARY PROBLEMS

defined by two different field distributions,

# 1

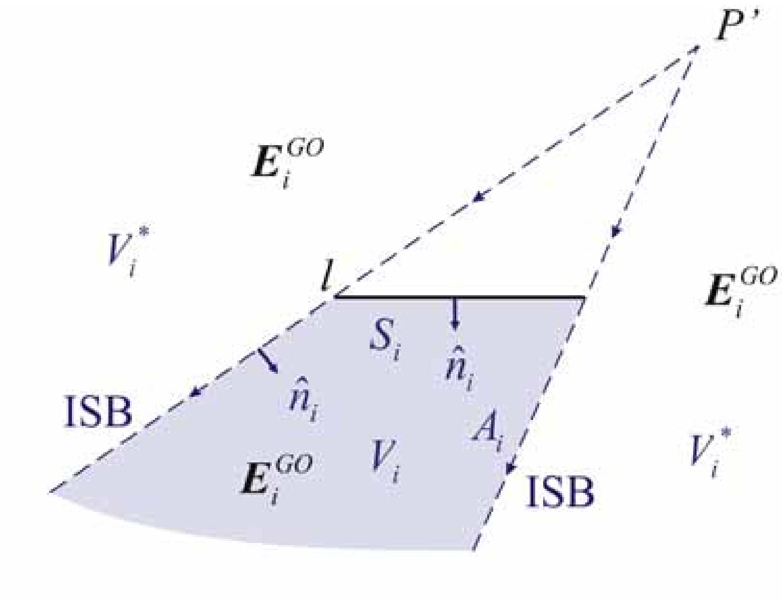


# 1 the GO incident field in absence of the scatterer;

# 2

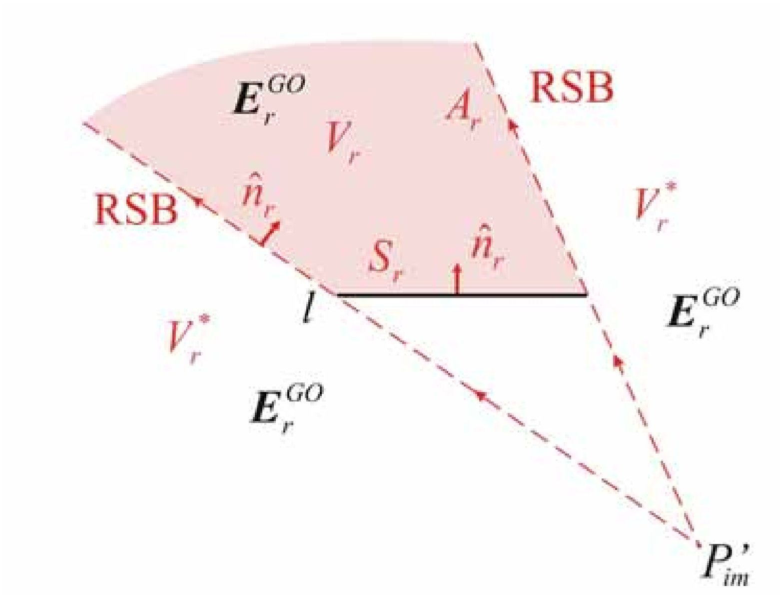


# 2 the analytical continuation in the whole space of the optical field from the image source (→ of the GO reflected field).

- the point-source is assumed not extremely close to the surface (→ reactive near field components can be neglected)

# SOLUTION TO THE AUXILIARY PROBLEMS

# 1

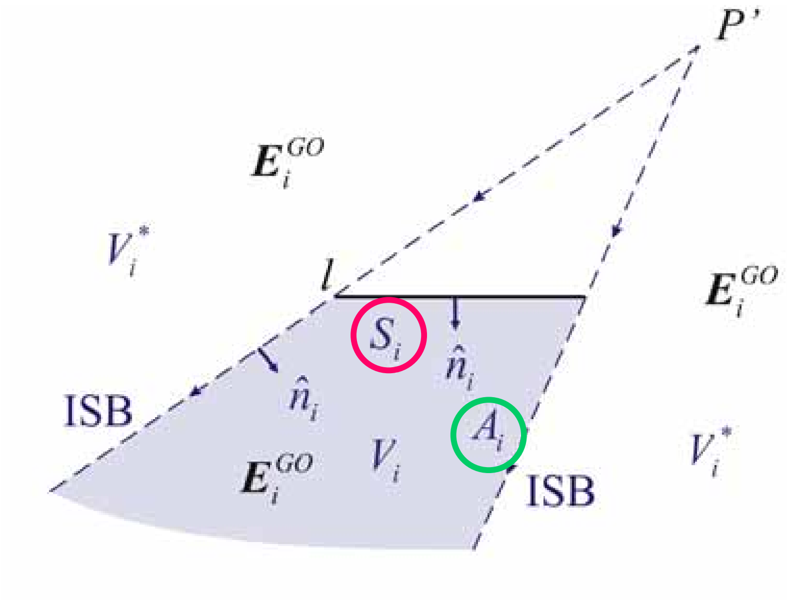


# 2

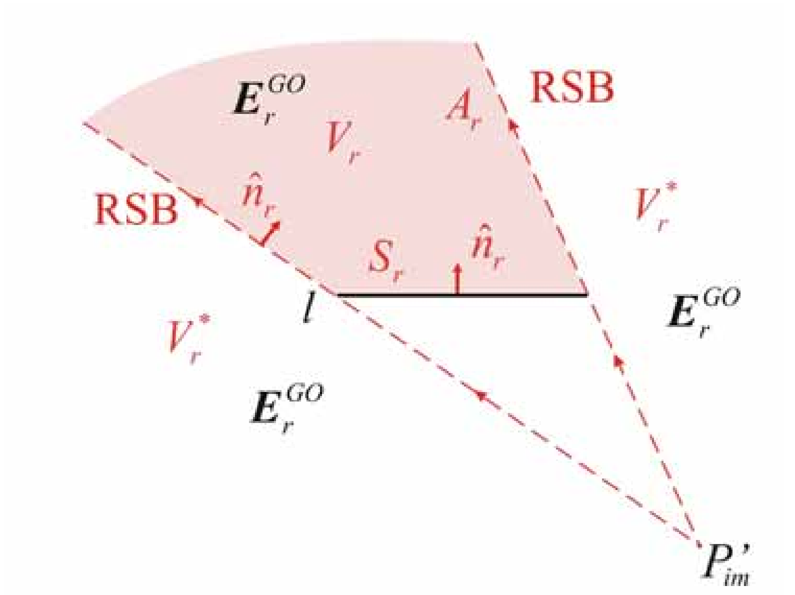


The **equivalence principle** is applied to each individual problem, and yields

$$\boldsymbol{E}_i^S(\boldsymbol{r}) + \boldsymbol{E}_i^A(\boldsymbol{r}) \approx \boldsymbol{E}_i^{GO}(\boldsymbol{r})U_i(\boldsymbol{r})$$

flat plate surface

truncated SB cone surface

$$U_{i,r}(\boldsymbol{r}) = \begin{cases} 1 & \boldsymbol{r} \in V_{i,r} \\ 0 & \boldsymbol{r} \in V_{i,r}^* \end{cases}$$

$$\boldsymbol{E}_r^S(\boldsymbol{r}) + \boldsymbol{E}_r^A(\boldsymbol{r}) \approx \boldsymbol{E}_r^{GO}(\boldsymbol{r})U_r(\boldsymbol{r})$$

the GO field is not an **exact**, but an **asymptotic** solution of Maxwell's equations inside $V_{i,r}$

# RECONSTRUCTION OF PO CURRENTS

# 1

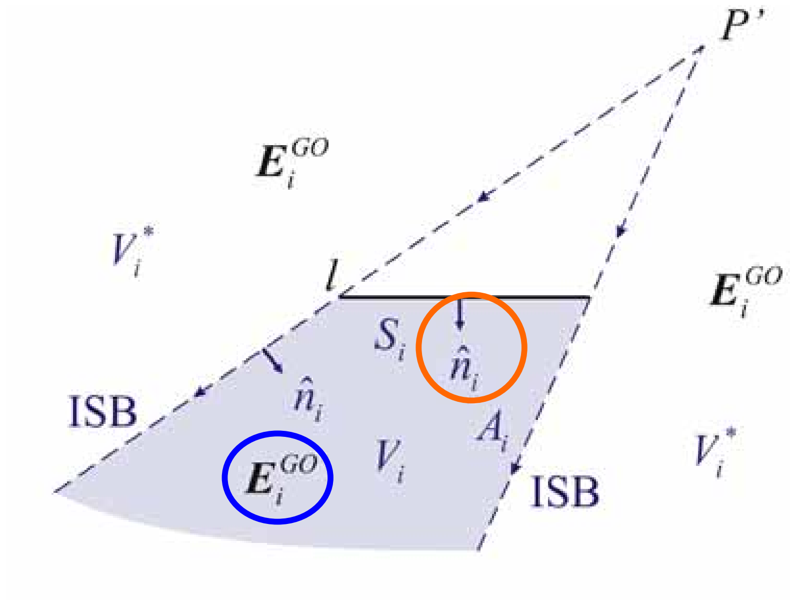


# 2

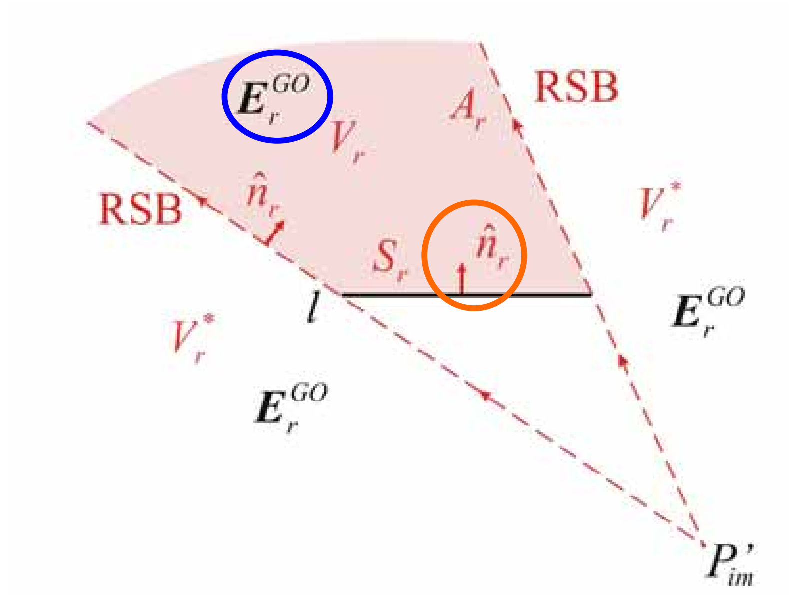


equivalent electric and magnetic currents over the plate, associated to GO fields

$$\boldsymbol{J}_i(\boldsymbol{r}_s) = \hat{n}_i \times \boldsymbol{H}_i^{GO}(\boldsymbol{r}_s)$$

$$\boldsymbol{M}_i(\boldsymbol{r}_s) = \boldsymbol{E}_i^{GO}(\boldsymbol{r}_s) \times \hat{n}_i$$

$$\boldsymbol{J}_r(\boldsymbol{r}_s) = \hat{n}_r \times \boldsymbol{H}_r^{GO}(\boldsymbol{r}_s) = \hat{n}_r \times \boldsymbol{H}_i^{GO}(\boldsymbol{r}_s)$$

$$\boldsymbol{M}_r(\boldsymbol{r}_s) = \boldsymbol{E}_r^{GO}(\boldsymbol{r}_s) \times \hat{n}_r = -\boldsymbol{E}_i^{GO}(\boldsymbol{r}_s) \times \hat{n}_r$$

b.c. on the p.e.c. surface

$$\hat{n}_r = -\hat{n}_i$$

$$\boldsymbol{J}_r(\boldsymbol{r}_s) - \boldsymbol{J}_i(\boldsymbol{r}_s) = 2\hat{n}_r \times \boldsymbol{H}_i^{GO}(\boldsymbol{r}_s)$$

$$\boldsymbol{M}_r(\boldsymbol{r}_s) - \boldsymbol{M}_i(\boldsymbol{r}_s) = 0$$

**PO currents (under GO approximation)**

$$\boldsymbol{J}^{PO}(\boldsymbol{r}') = 2\hat{n} \times \boldsymbol{H}_i(\boldsymbol{r}') \simeq 2\hat{n} \times \boldsymbol{H}_i^{GO}(\boldsymbol{r}')$$

# RECONSTRUCTION OF PO FIELD

# 1

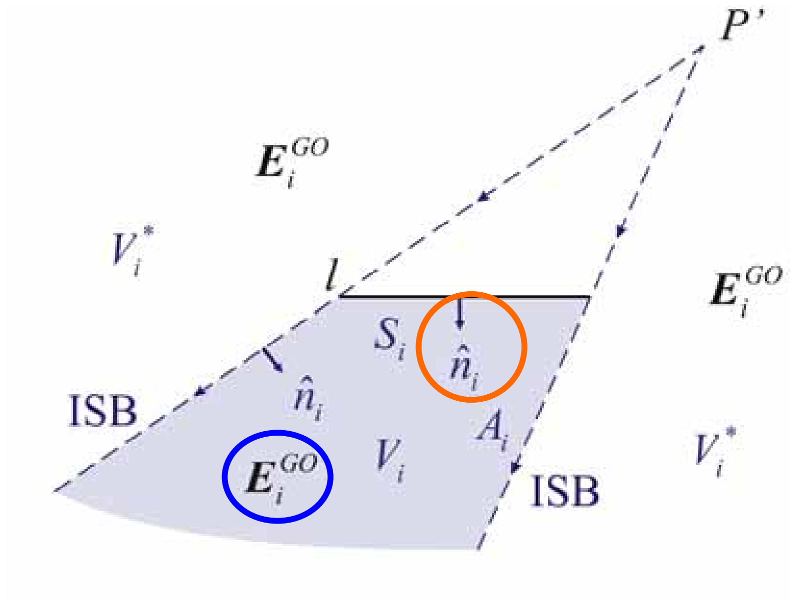


# 2

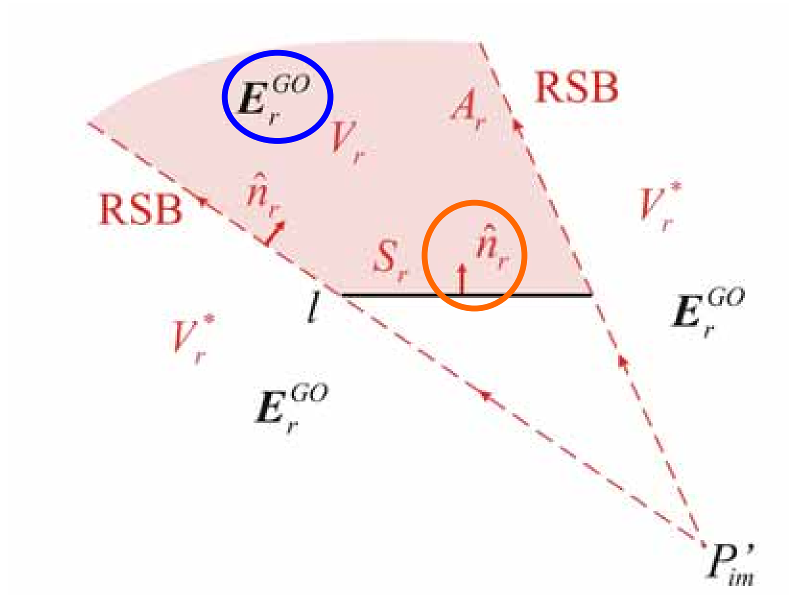


- The PO currents are defined here under **locally plane wave (GO)** approximation

$$\boldsymbol{J}^{PO}(\boldsymbol{r}') \simeq 2\hat{n} \times \boldsymbol{H}_i^{GO}(\boldsymbol{r}')$$

asymptotically coincident with

$$\boldsymbol{J}^{PO}(\boldsymbol{r}') = 2\hat{n} \times \boldsymbol{H}_i(\boldsymbol{r}')$$

**in absence of reactive primary field**

- Combining the two solutions…

$$\boxed{\boldsymbol{E}^{PO}(\boldsymbol{r}) = \boldsymbol{E}_r^S(\boldsymbol{r}) - \boldsymbol{E}_i^S(\boldsymbol{r})}$$

→ the minus compensates for the reversing normal ( $\hat{n}$ defining the PO currents is that emerging from the ***lit*** side of the scatterer, as in **#2**)

# ASYMPTOTIC REPRESENTATION OF THE PO FIELD

$$\boldsymbol{E}^{PO} = \boldsymbol{E}_r^S - \boldsymbol{E}_i^S =$$
$$\approx -\boldsymbol{E}_r^A + \boldsymbol{E}_i^A + \boldsymbol{E}_r^{GO} U_r - \boldsymbol{E}_i^{GO} U_i$$

**PO back-radiation**
(asympt. cancels the GO incident field beyond the plate)

difference between PO and GO fields

→ **diffracted field** in the PO assumption

An analogous identity holds for the magnetic field

- The radiation integrals on the SB's can be exactly represented as line integrals along the contour which bounds the flat facet

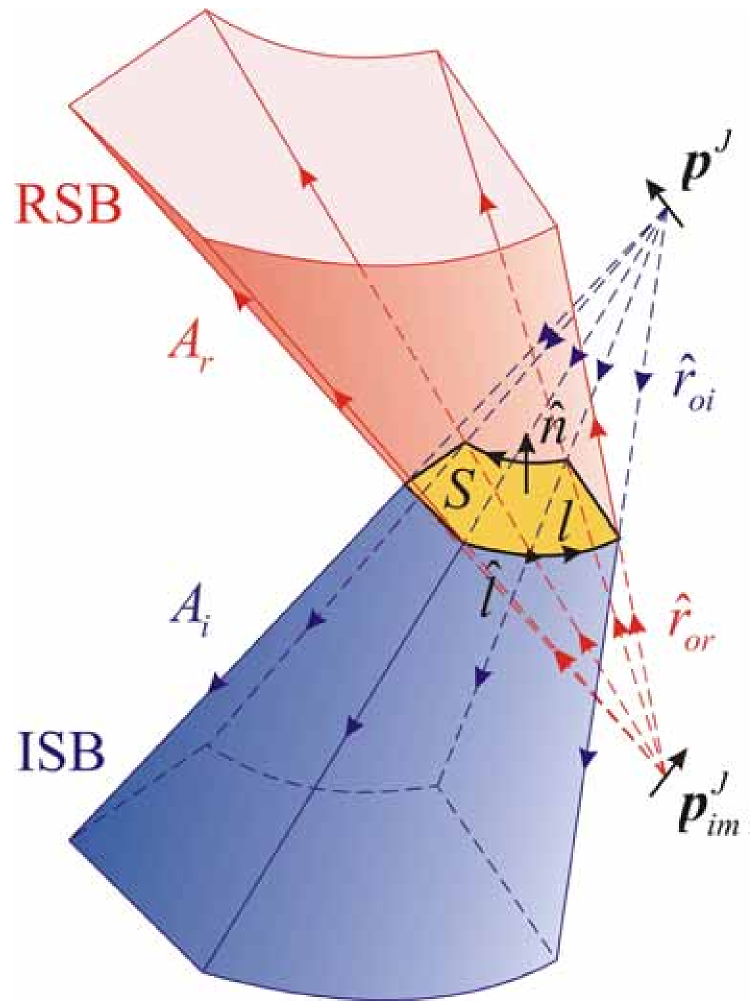

# EVALUATION OF THE CONICAL SB CONTRIBUTIONS

- Let us refer to $\boldsymbol{E}_r^A$ ; the same treatment also applies to $\boldsymbol{E}_i^A$

$$\boldsymbol{E}_r^A(\boldsymbol{r}) = \iint_{A_r} -j\frac{\zeta}{k}\nabla\times\nabla\times\underbrace{\left(\hat{n}_r\times\boldsymbol{H}_r^{GO}(\boldsymbol{r}'')\right)}_{\boldsymbol{J}_r} - \nabla\times\underbrace{\left(\boldsymbol{E}_r^{GO}(\boldsymbol{r}'')\times\hat{n}_r\right)}_{\boldsymbol{M}_r}\frac{e^{-jkR}}{4\pi R}\,\mathrm{d}A_r$$

- Both the electric and magnetic **GO equivalent currents** are parallel to the local reflected ray direction $\hat{r}_r^o$

- They maintain the spherical wave structure of the GO fields

→ **linear phase progression**, along the reflected ray-paths originating at the image source-point, **with the propagation wave-number of the surrounding medium**

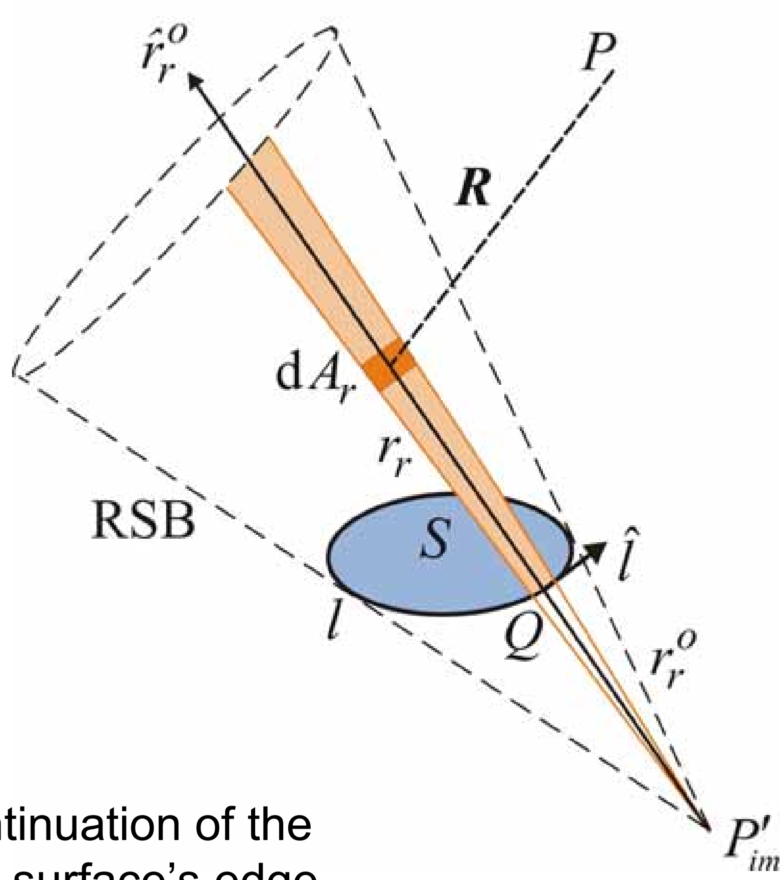


$$\boldsymbol{J}_r(\boldsymbol{r}'') = J_r(\boldsymbol{r}''_Q)\frac{r_r^o}{r_r}e^{-jk\left(r_r - r_r^o\right)}\hat{r}_r^o$$

ray-optical continuation of the currents at the surface's edge

$\frac{r_r^o}{r_r}$ → spreading factor of diverging rays

# PARAMETRIZATION OF THE SB INTEGRALS

As suggested by the features of the GO equivalent currents

- Both the SB cones are parameterized into **elemental semi-infinite trapezoidal strips** from a point on the surface rim to infinity, parallel to the local reflected ray direction

- The elemental area on the conical RSB is bounded by two neighboring diverging reflected **ray-paths**, and by two subsequent reflected spherical **wave-fronts**

$$\mathrm{d}A_r = \frac{r_r}{r_r^o}\left|\hat{r}_r^o \times \hat{\ell}\right| \mathrm{d}r_r\, \mathrm{d}\ell$$

widening factor of diverging strip

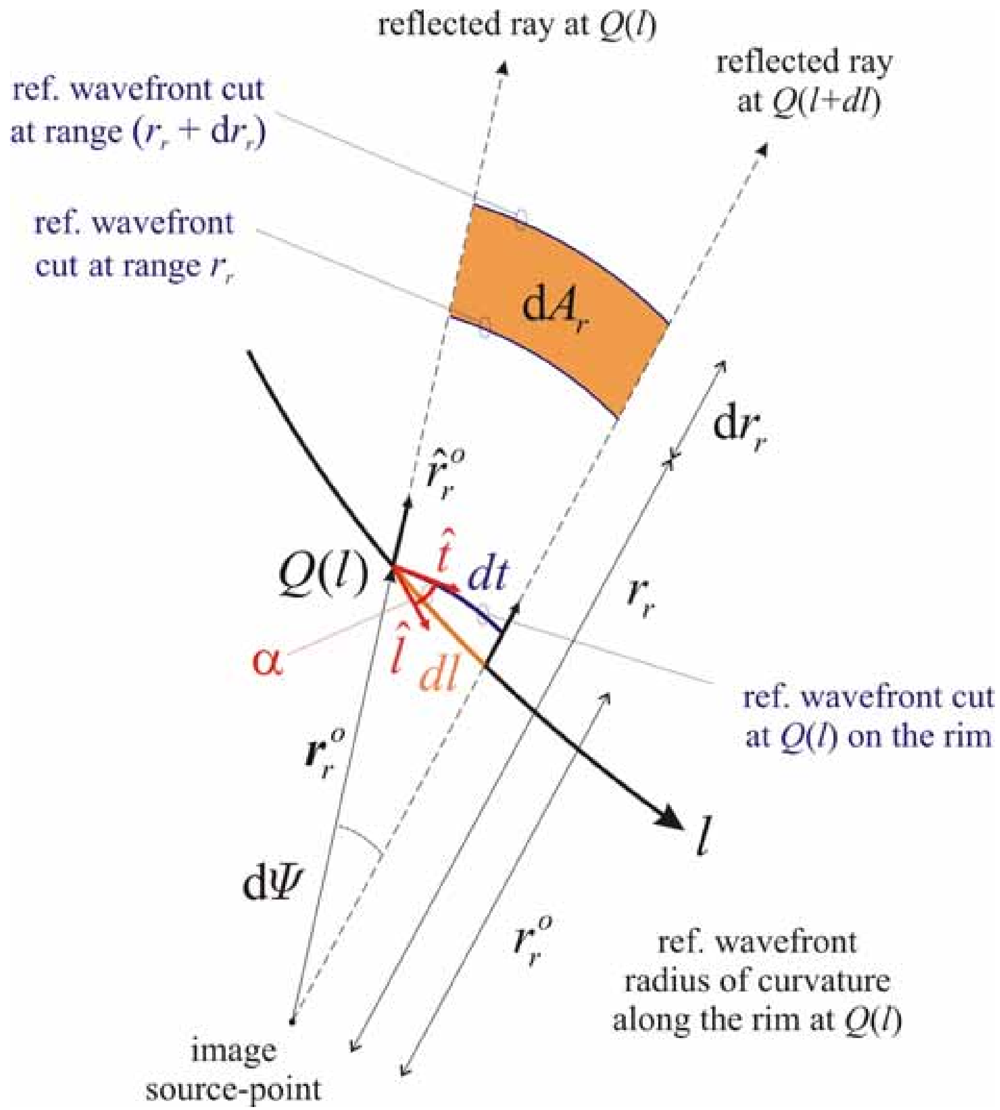

# ELEMENTAL STRIPS' RADIATION

- The radiation integral on the RSB is split up into sequential line integrals along the elemental ray-directed strips and along the closed contour of the plate rim

$$\iint_{A_r} (\ldots)\, \mathrm{d}A_r = \oint_{\ell} \underbrace{\int_{r_r^o}^{\infty} (\ldots) \frac{r_r}{r_r^o} \left| \hat{r}_r^o \times \hat{\ell} \right| \mathrm{d}r_r}_{\text{incremental field of the elemental semi-infinite strip}} \mathrm{d}\ell$$

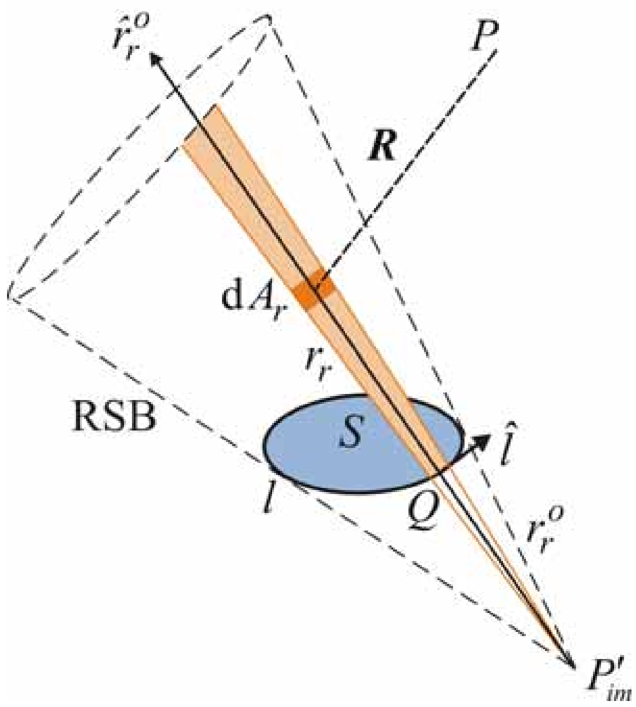


- Due to
  - → the properties of the GO equivalent currents ( $// \hat{r}_r^o$ ; phase progression with *k*)
  - → the cancellation between the spherical-wave spreading factor of the GO field and the widening factor of the elemental strip

→ **The integration in the strips' direction can be performed in exact closed form**

# EXACT INTEGRATION

- The integral (common to the radiation of both electric and magnetic currents)

$$\boxed{\int_{r_r^o}^{\infty} \nabla \times \left\{ \frac{e^{-jkR}}{4\pi R} e^{-jk\left(r_r - r_r^o\right)} \hat{r}_r^o \right\} \mathrm{d}r_r = \frac{e^{-jkR_0}}{4\pi R_0} \cot\frac{\theta_{sr}}{2} \hat{\phi}_{sr}}$$

only yields a contribution from the strip's end-point *Q*

- Local spherical reference system with origin at the end point *Q* of each strip, and *z*-axis parallel to the reflected ray-path

$$\boldsymbol{R}_0 = \boldsymbol{r} - \boldsymbol{r}_Q$$

$$\hat{\phi}_{sr} = \frac{\hat{r}_r^o \times \hat{R}_0}{\left|\hat{r}_r^o \times \hat{R}_0\right|}$$

$$\hat{\theta}_{sr} = \hat{\phi}_{sr} \times \hat{R}_0$$

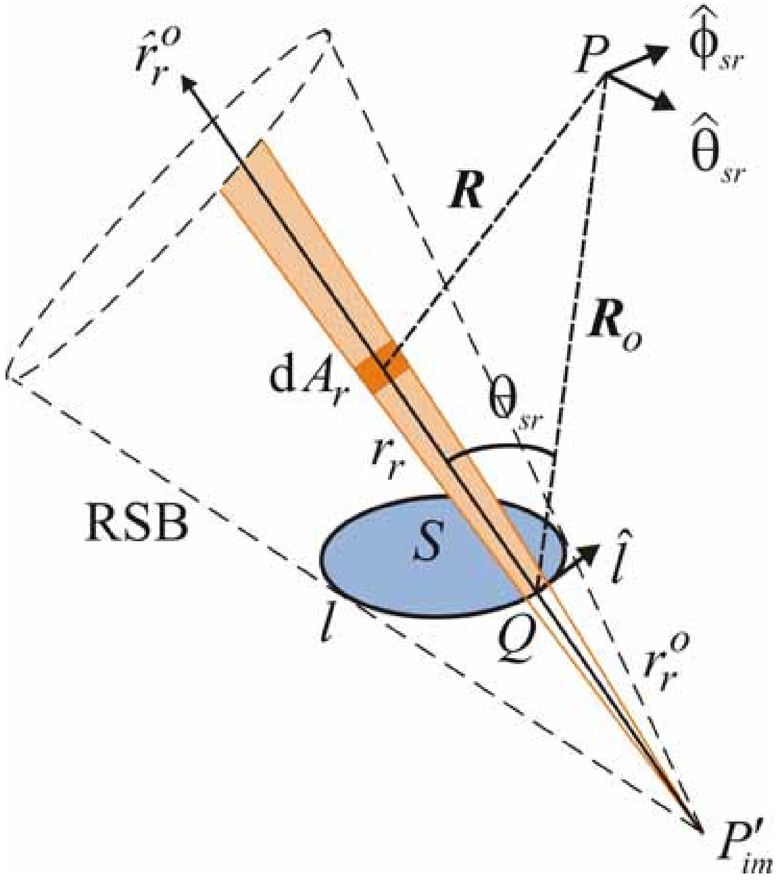

# LINE INTEGRAL REPRESENTATION

The electric and magnetic fields radiated by the equivalent currents on the SB are expressed as **line integrals** along the rim contour of the scattering surface

$$\boldsymbol{E}_r^A = \oint_\ell \left\{ \boldsymbol{e}_r^J(\ell) + \boldsymbol{e}_r^M(\ell) \right\} \mathrm{d}\ell \qquad \boldsymbol{H}_r^A = \oint_\ell \left\{ \boldsymbol{h}_r^J(\ell) + \boldsymbol{h}_r^M(\ell) \right\} \mathrm{d}\ell$$

$$\begin{Bmatrix} \boldsymbol{e}_r^J(\ell) \\ \boldsymbol{h}_r^M(\ell) \end{Bmatrix} = \begin{Bmatrix} -\zeta\, \boldsymbol{H}_r^{GO}(\ell)\cdot\hat{\ell} \\ \zeta^{-1}\boldsymbol{E}_r^{GO}(\ell)\cdot\hat{\ell} \end{Bmatrix} \frac{e^{-jkR_0}}{4\pi R_0} \left( -\frac{\hat{R}_0}{jkR_0} + \cot\frac{\theta_{sr}}{2}\,\hat{\theta}_{sr} \right)$$

$$\begin{Bmatrix} \boldsymbol{e}_r^M(\ell) \\ \boldsymbol{h}_r^J(\ell) \end{Bmatrix} = -\begin{Bmatrix} \boldsymbol{E}_r^{GO}(\ell)\cdot\hat{\ell} \\ \boldsymbol{H}_r^{GO}(\ell)\cdot\hat{\ell} \end{Bmatrix} \frac{e^{-jkR_0}}{4\pi R_0} \cot\frac{\theta_{sr}}{2}\,\hat{\phi}_{sr}$$

**dominant asymptotic contributions**

**fields of equivalent electric and magnetic dipoles, parallel to the reflected ray direction, with modified pattern**

# INCREMENTAL FIELDS

- The amplitude of the incremental field radiated by each elemental strip is proportional to the exciting GO field at the plate's rim

- The pattern of the incremental field has a dominant asymptotic contribution given by ***cot ($\theta_{sr}$/ 2)***

→ each incremental field is **singular** along the strip direction itself ( $\theta_{sr} = 0$ → $\boldsymbol{r} - \boldsymbol{r}_Q \,//\, \boldsymbol{r}_Q - \boldsymbol{r}'$ )

- This singularity of the integrand function results in a **discontinuity** of the field $\left(\boldsymbol{E}_r^A, \boldsymbol{H}_r^A\right)$ after the integration along $\ell$

→ **compensates** for the abrupt **discontinuity** of the **GO reflected field** across the RSB (diffracted field)

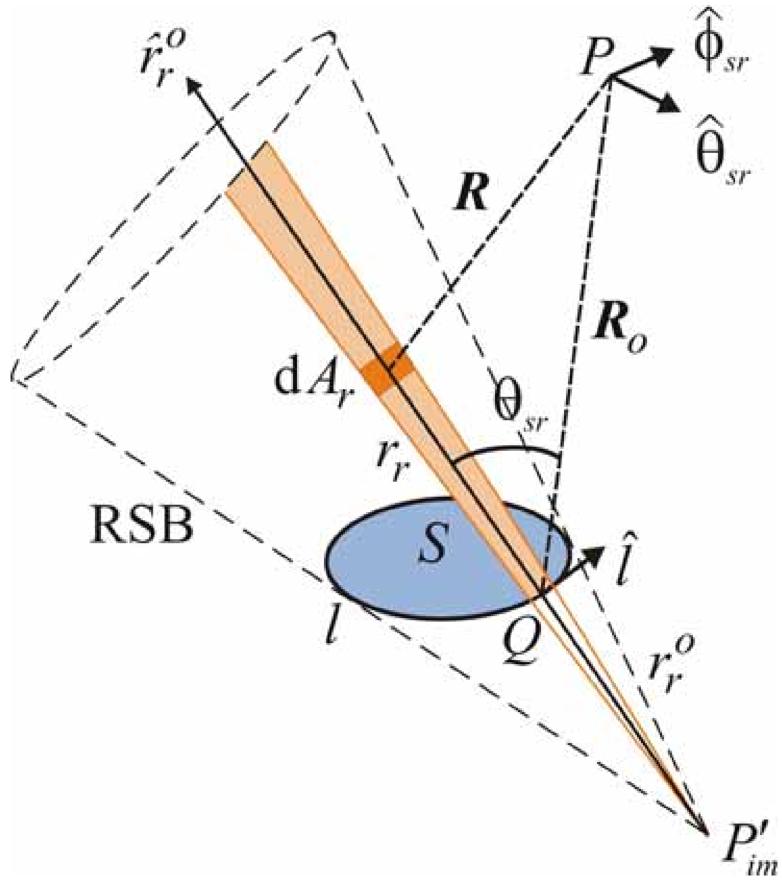

# FIELDS FROM THE ISB

- The same treatment can be applied to the field contributions $\left(\boldsymbol{E}_i^A, \boldsymbol{H}_i^A\right)$, radiated by the GO equivalent currents on the incidence SB

$$\boldsymbol{E}_i^A = \oint_\ell \left\{ \boldsymbol{e}_i^J(\ell) + \boldsymbol{e}_i^M(\ell) \right\} \mathrm{d}\ell \qquad \boldsymbol{H}_i^A = \oint_\ell \left\{ \boldsymbol{h}_i^J(\ell) + \boldsymbol{h}_i^M(\ell) \right\} \mathrm{d}\ell$$

$$\begin{Bmatrix} \boldsymbol{e}_i^J(\ell) \\ \boldsymbol{h}_i^M(\ell) \end{Bmatrix} = \begin{Bmatrix} \zeta\, \boldsymbol{H}_i^{GO}(\ell)\cdot\hat{\ell} \\ -\zeta^{-1}\boldsymbol{E}_i^{GO}(\ell)\cdot\hat{\ell} \end{Bmatrix} \frac{e^{-jkR_0}}{4\pi R_0} \left( -\frac{\hat{R}_0}{jkR_0} + \cot\frac{\theta_{si}}{2}\,\hat{\theta}_{si} \right)$$

$$\begin{Bmatrix} \boldsymbol{e}_i^M(\ell) \\ \boldsymbol{h}_i^J(\ell) \end{Bmatrix} = \begin{Bmatrix} \boldsymbol{E}_i^{GO}(\ell)\cdot\hat{\ell} \\ \boldsymbol{H}_i^{GO}(\ell)\cdot\hat{\ell} \end{Bmatrix} \frac{e^{-jkR_0}}{4\pi R_0} \cot\frac{\theta_{si}}{2}\,\hat{\phi}_{si}$$

- Local spherical reference system with origin at any point $Q$ on the plate's rim, and $z$-axis parallel to the incident ray-path

$$\boldsymbol{R}_0 = \boldsymbol{r} - \boldsymbol{r}_Q; \qquad \hat{\phi}_{si} = \frac{\hat{r}_i^o \times \hat{R}_0}{\left|\hat{r}_i^o \times \hat{R}_0\right|}; \qquad \hat{\theta}_{si} = \hat{\phi}_{si} \times \hat{R}_0$$

- Sign reversal because of opposite normals in auxiliary problems

# SBI REPRESENTATION OF THE PO FIELD

- Final **Shadow Boundary Integral (SBI)** representation of the PO field from a flat plate, for illuminating hertzian dipole,

$$\boxed{\begin{aligned}\boldsymbol{E}^{PO} \approx\ & \boldsymbol{E}_r^{GO} U_r - \boldsymbol{E}_i^{GO} U_i + \\ & - \oint_\ell \left\{ \boldsymbol{e}_r^J(\ell) + \boldsymbol{e}_r^M(\ell) \right\} \mathrm{d}\ell + \oint_\ell \left\{ \boldsymbol{e}_i^J(\ell) + \boldsymbol{e}_i^M(\ell) \right\} \mathrm{d}\ell\end{aligned}}$$

$\ell$ : plate's rim

+ **efficient**; surface-to-line integral reduction
+ **physically meaningful**; the near-field representation resembles the asymptotic description in optical regime

– fails at observation points extremely close to the surface; the equivalence principle is applied to the (non-Maxwellian) GO field

# PLANE-WAVE INCIDENCE

- The SBI formulation can be extended to treat plane-wave illumination
- The optical SB's are **cylinder-shaped** surfaces, whose axes are parallel to the aspects of the incident and reflected plane wave
- The SB's are parameterized into incremental semi-infinite strips, bounded by two neighbouring **parallel** incident or reflected rays
- Both the widening factor of the elemental strip on a SB and the spreading factor of the GO field (plane wave) are **unity** → cancellation
- The PO field is again described by the same expression, where the local spherical coordinate systems refer to *z*-axes that are parallel to

$$\hat{k}_i, \hat{k}_r$$

in place of

$$\hat{r}_i^o, \hat{r}_r^o$$

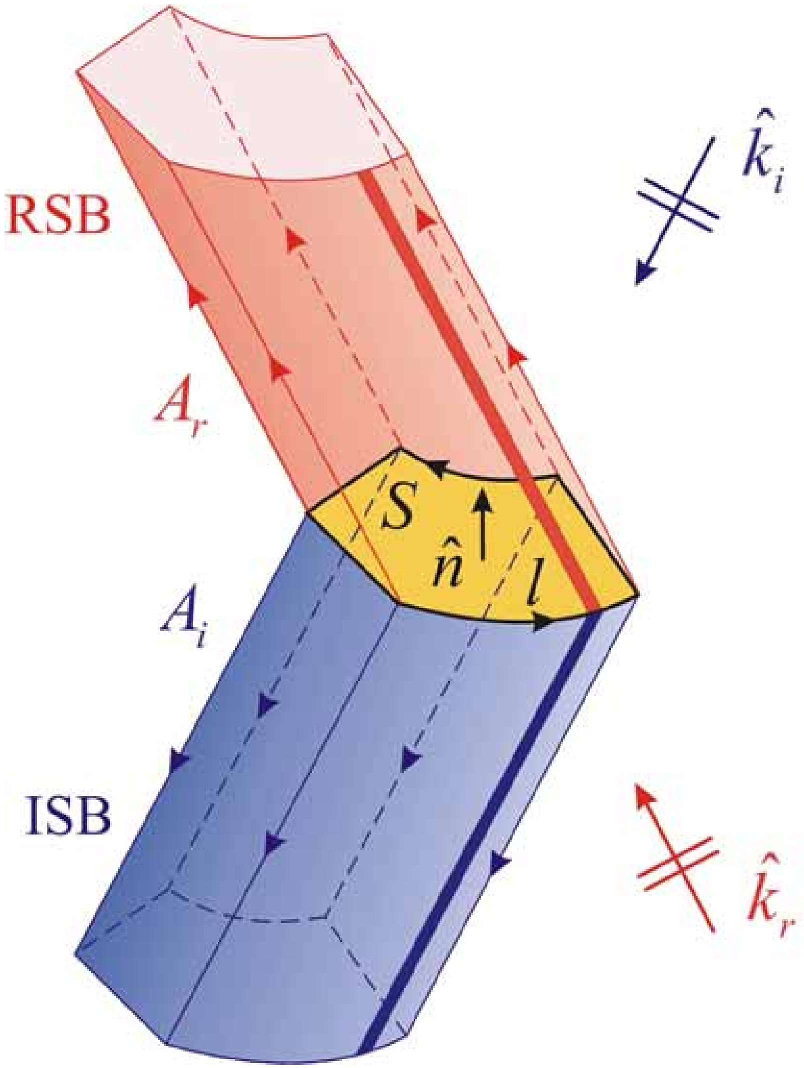

# SURFACE SEGMENTATION

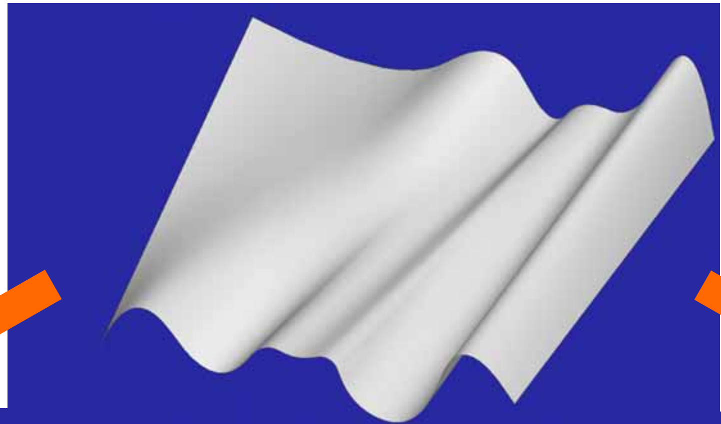

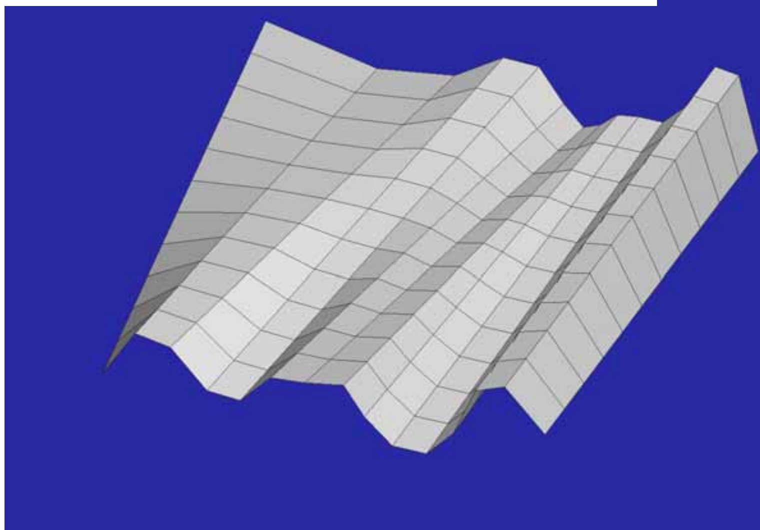

large facets

(phase error)

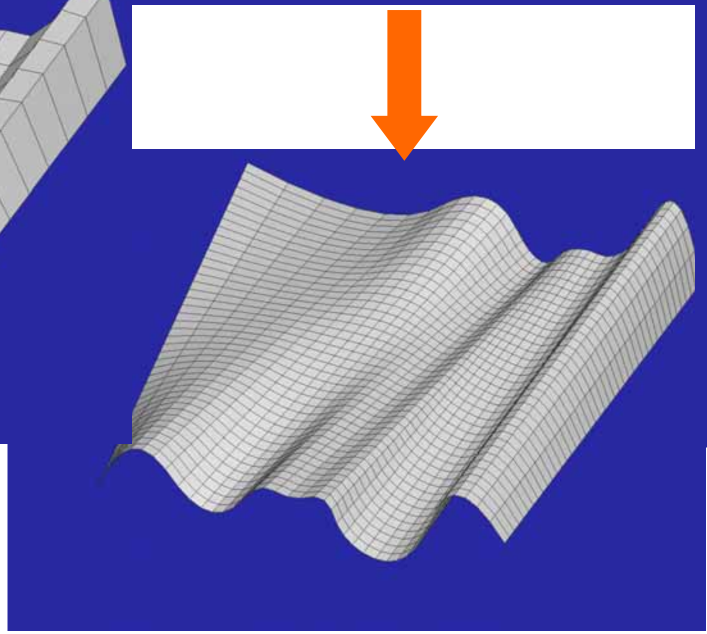

intermediate meshing

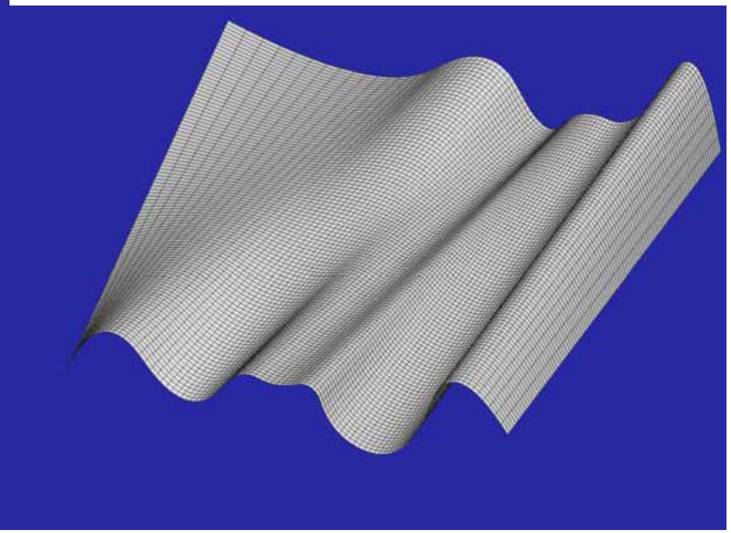

small facets

(quasi-numerical integration)

# NON-UNIFORM MESHING

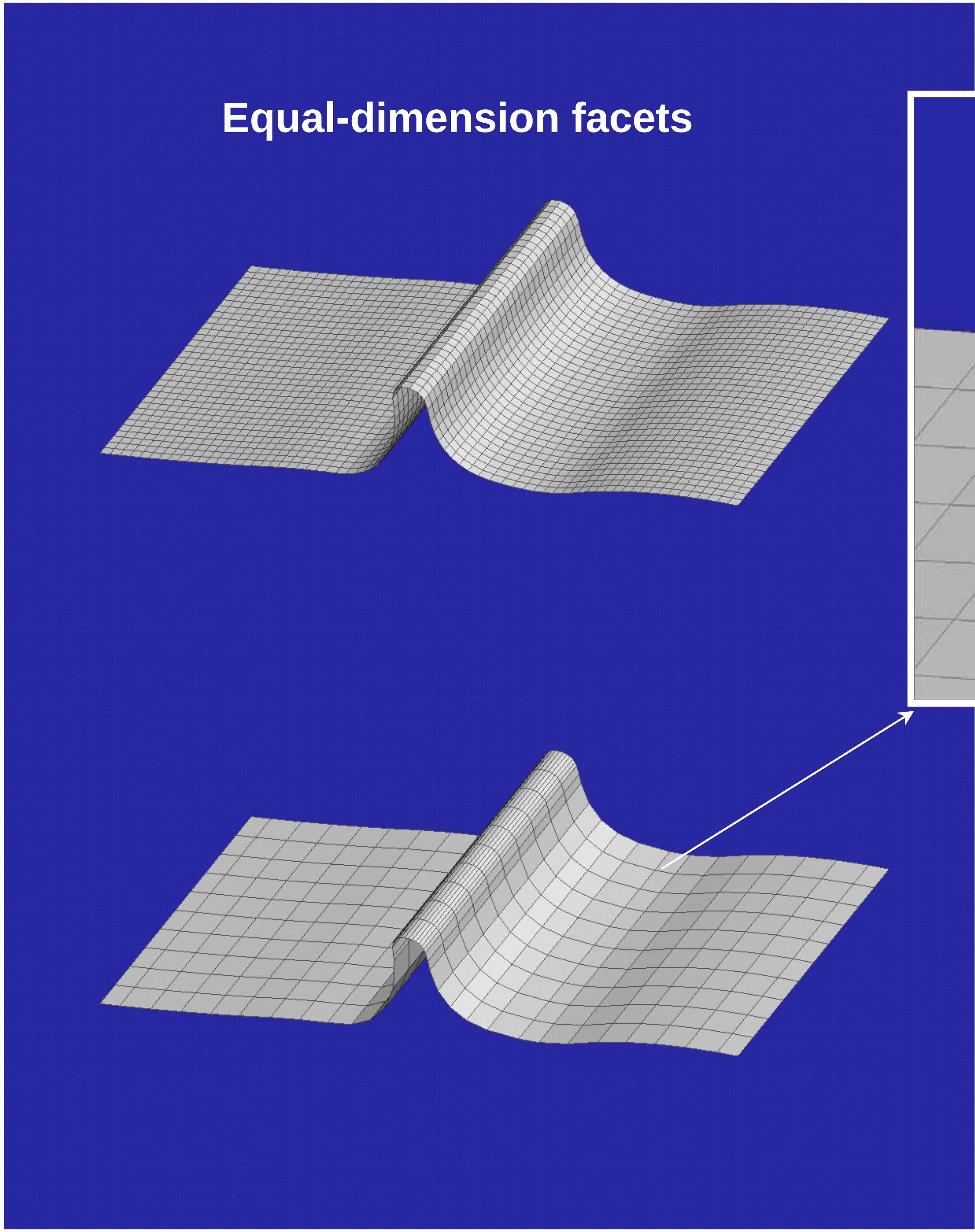


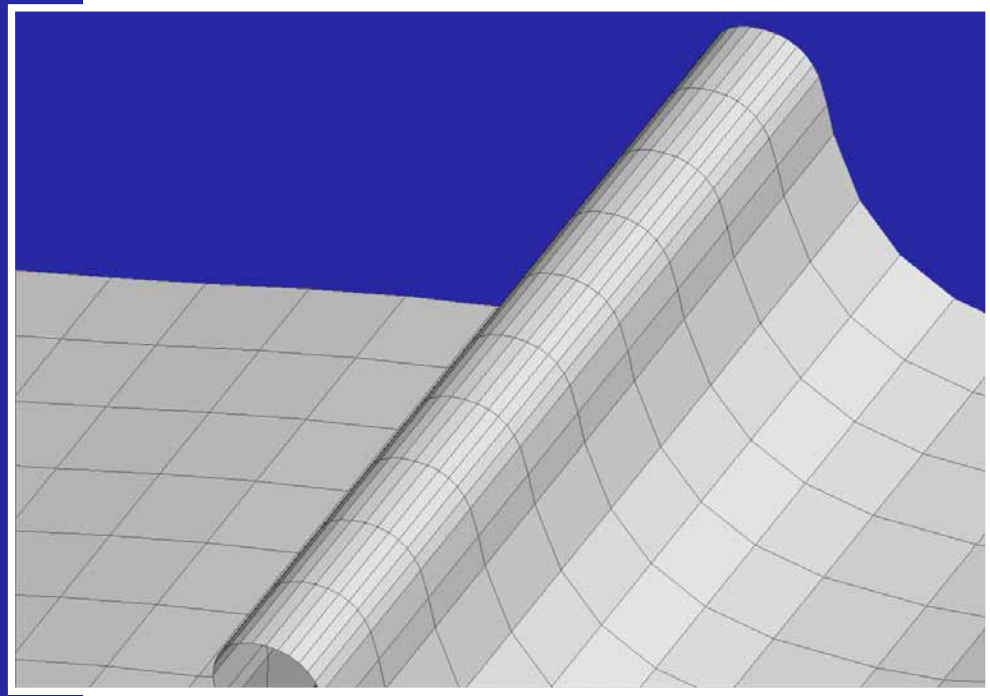

**The trade off between good approximation and computational efficiency is solved by a non-uniform meshing**

# TEST CASES

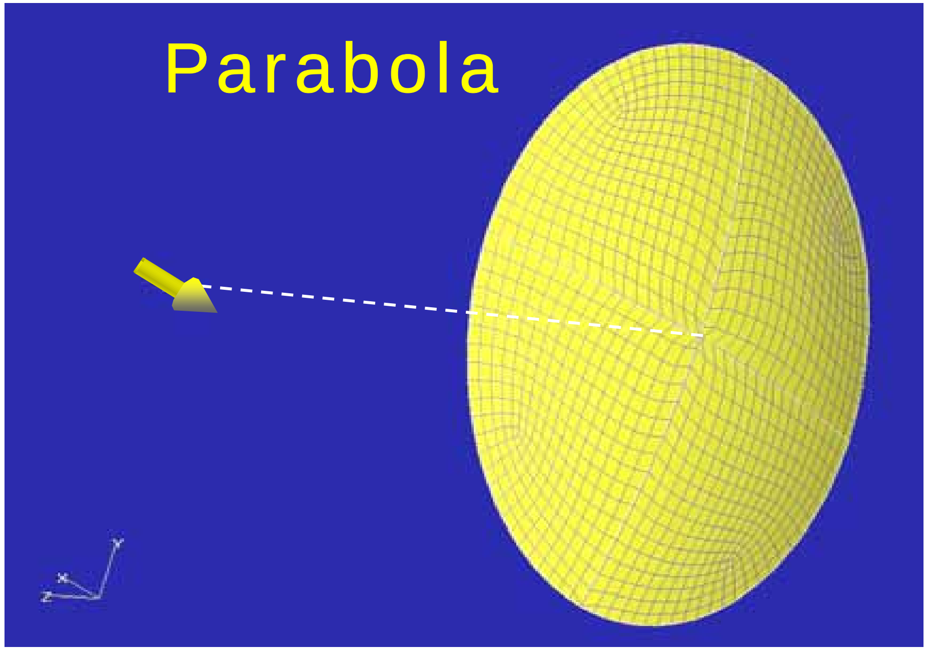


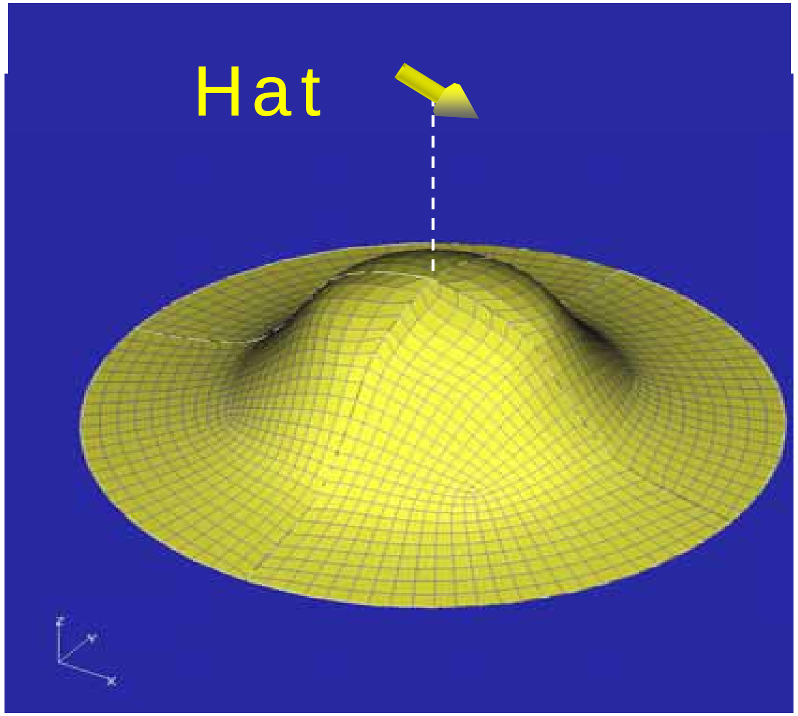


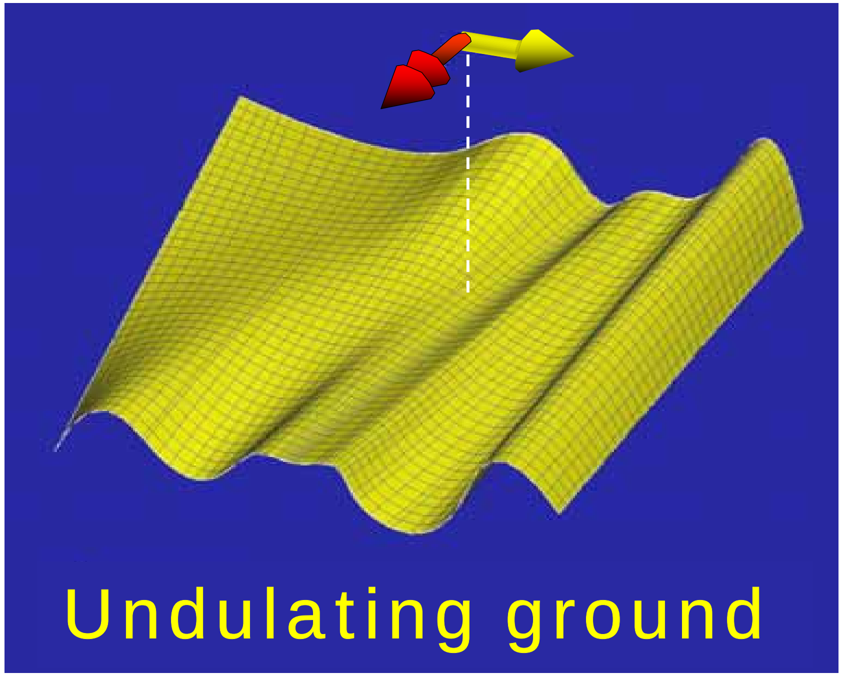


**increasing level of difficulty**

# NUMERICAL RESULTS

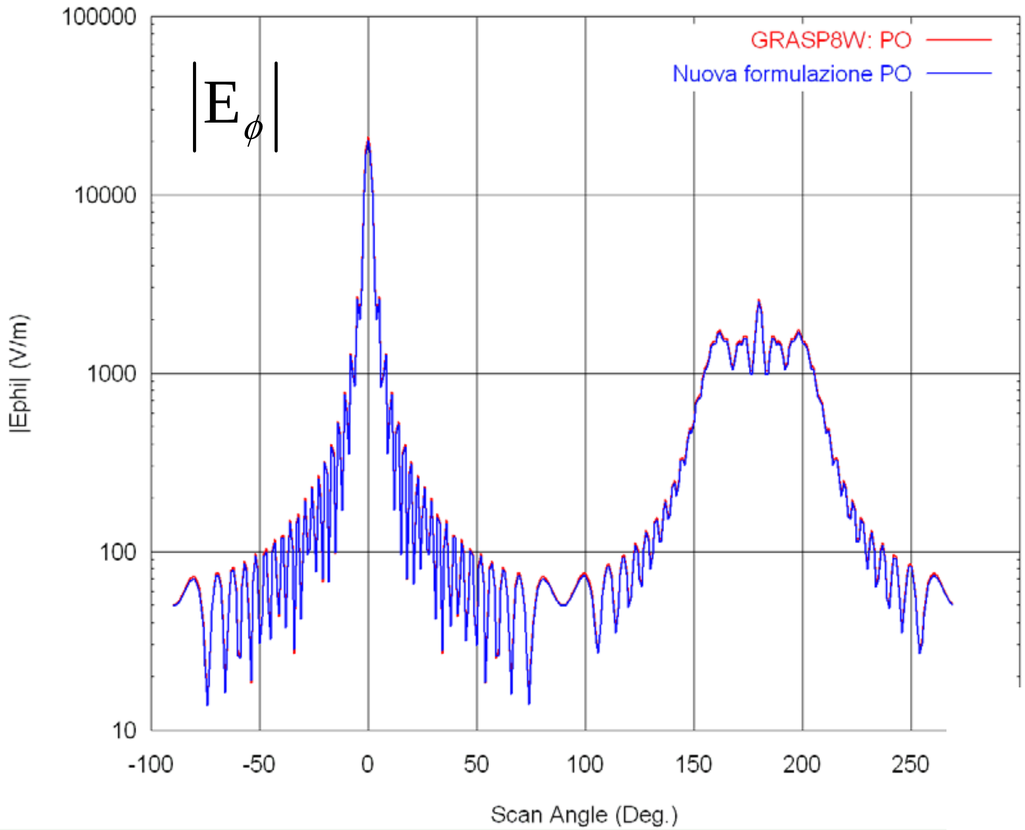


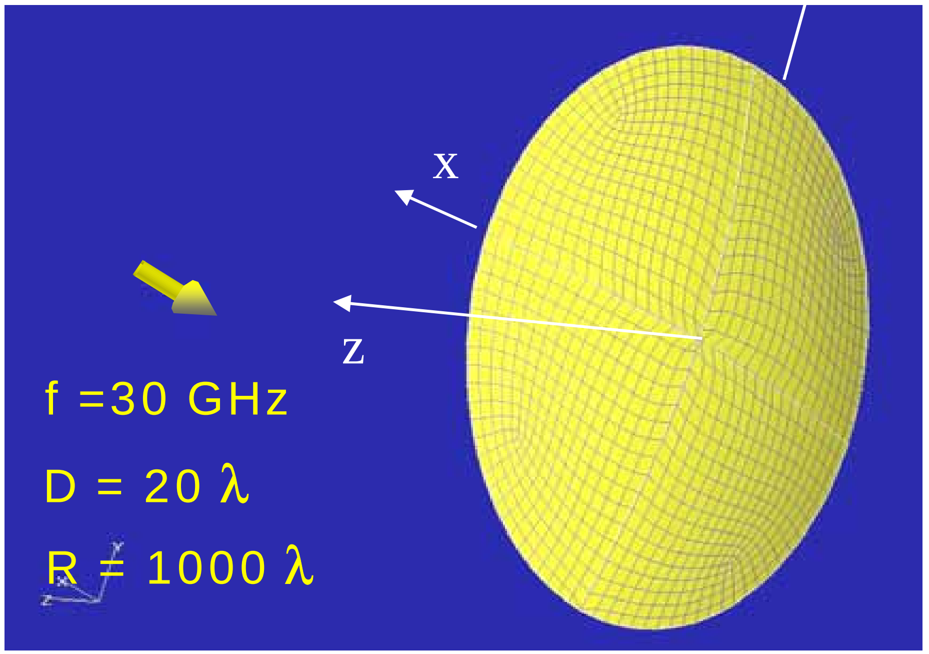


Mesh size < 3λ, with h = λ/50.

Number of facets: from 1116 to 3276 for D ranging from 20 to 100 λ.

Error less than 10% also for –40 dB level

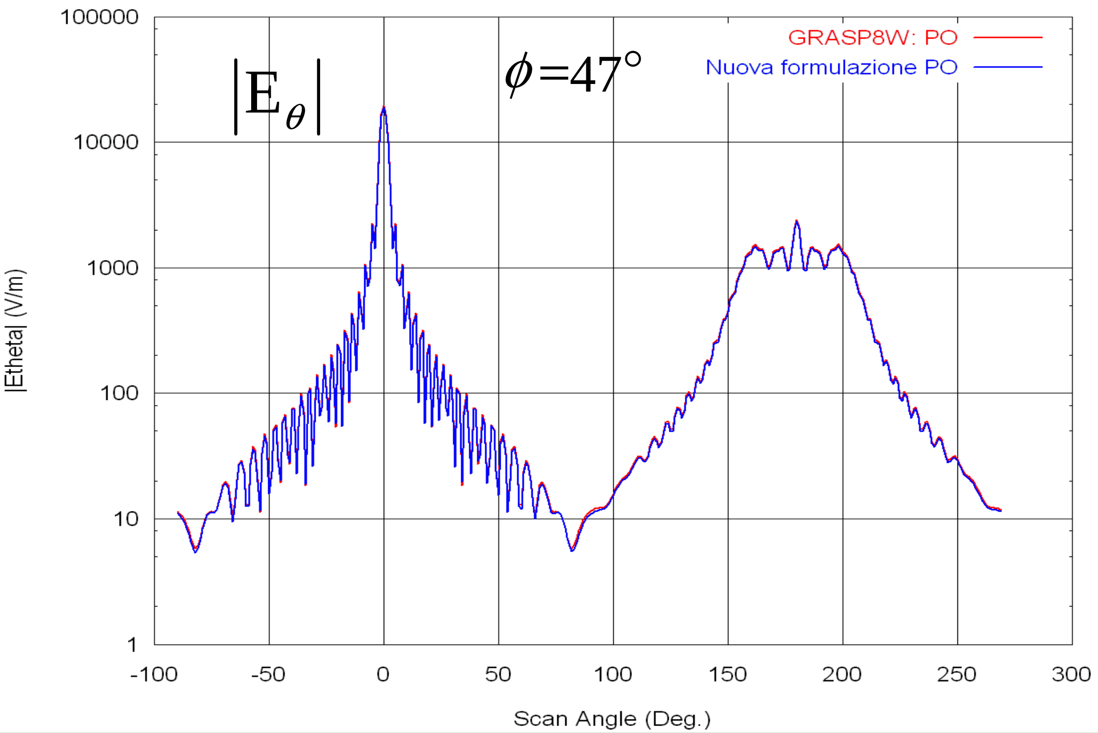

# NUMERICAL RESULTS

f =3 GHz

D = 14 λ

R = 8 λ

h = 10 λ

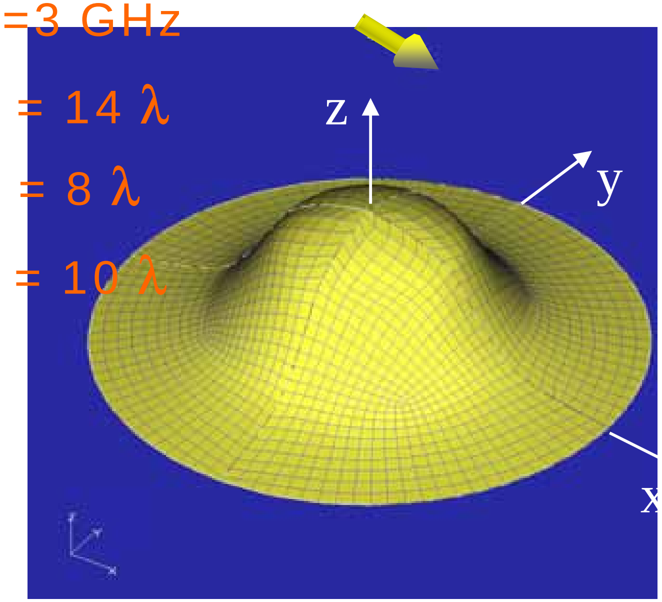


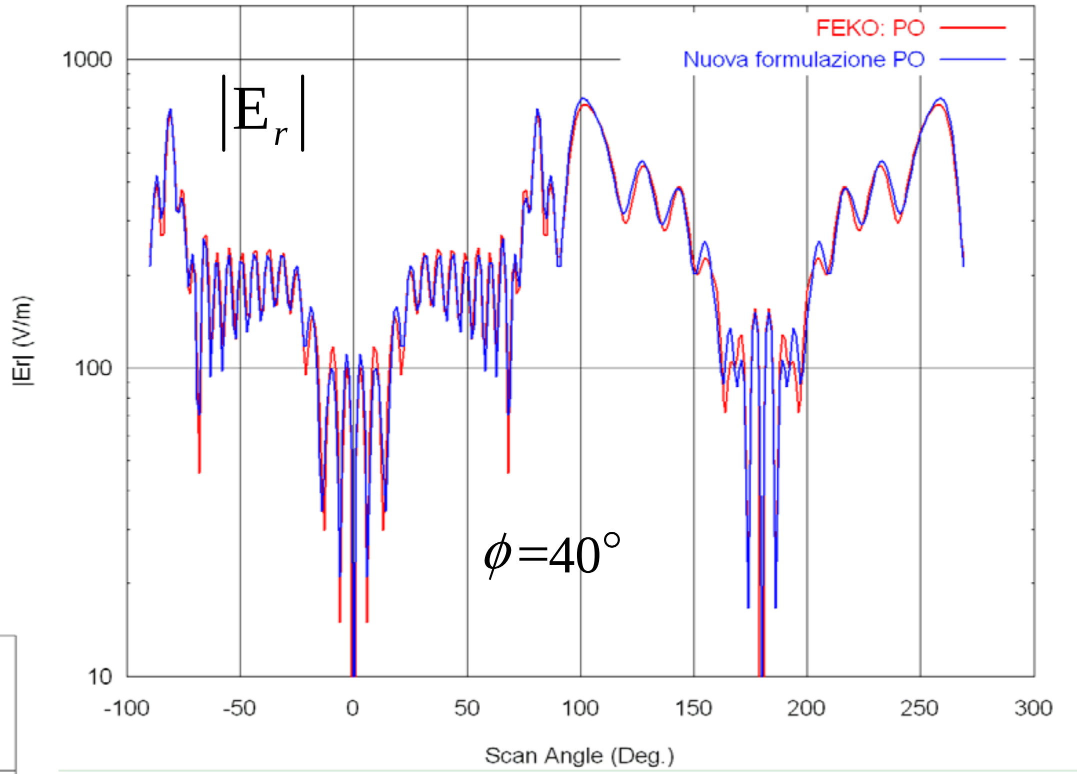


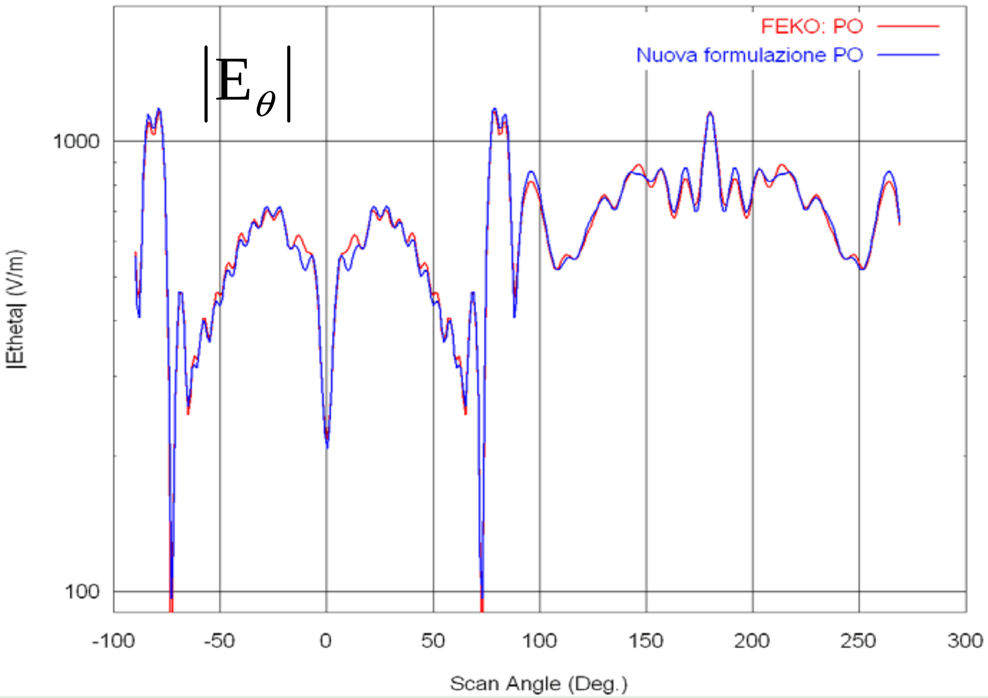


Mesh size < 2λ, with h = λ/50, R < 1/100

Error less than 10%

# NUMERICAL RESULTS

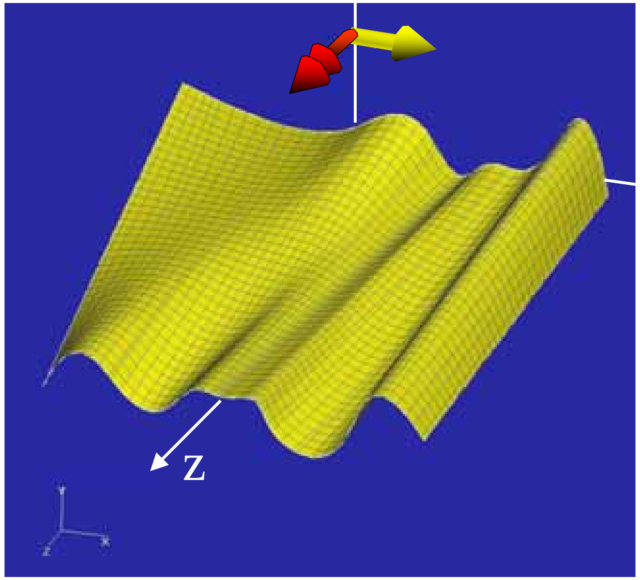


f =3 GHz

D = 10 λ X 8 λ

R = 30 λ

h = 20 λ

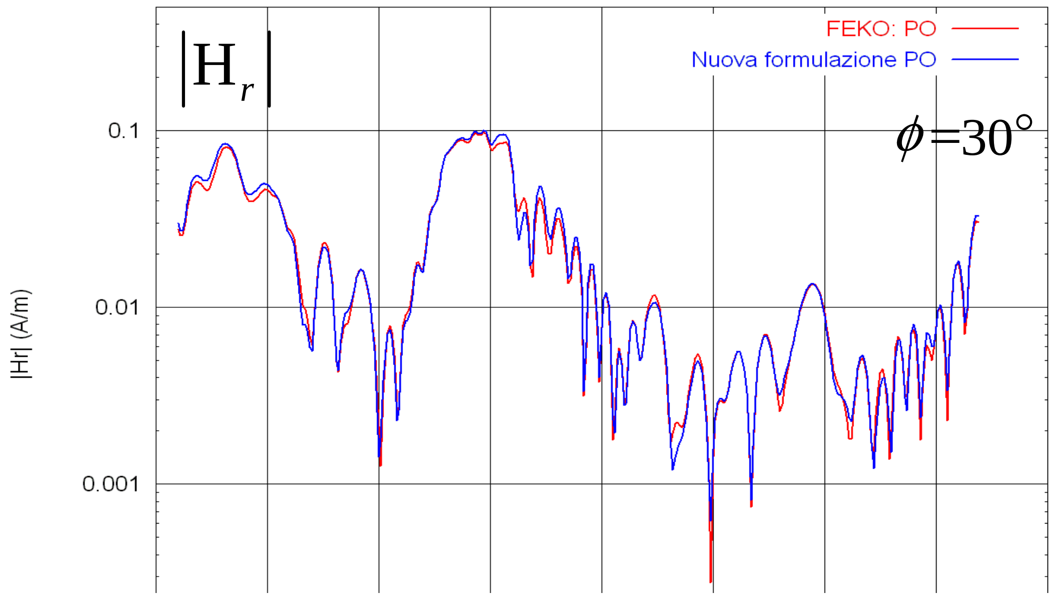


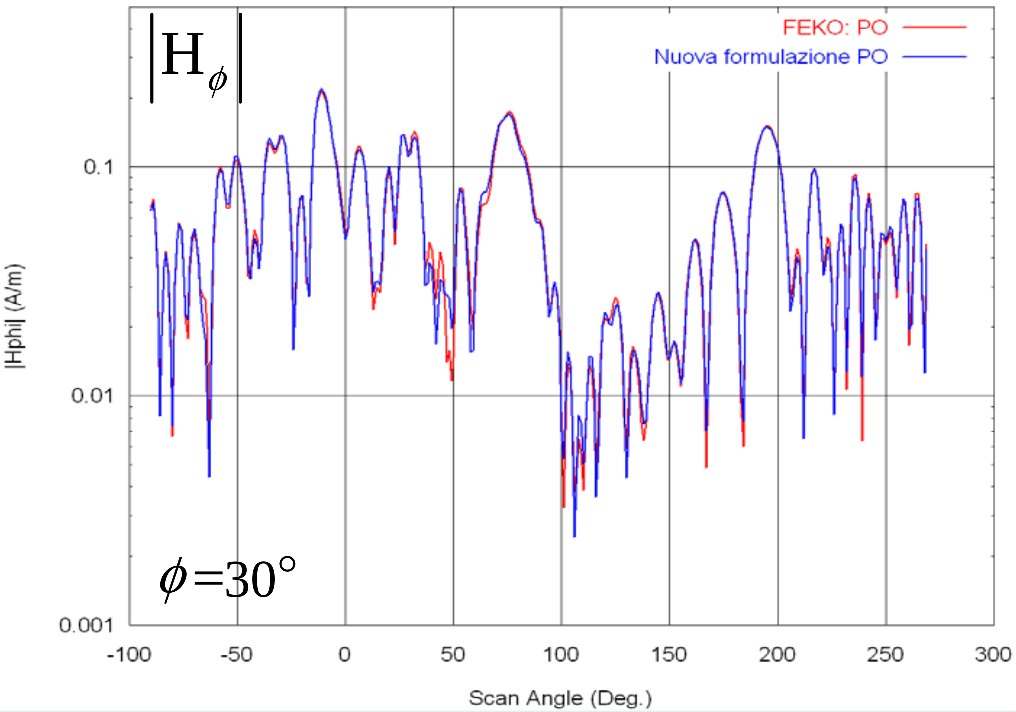


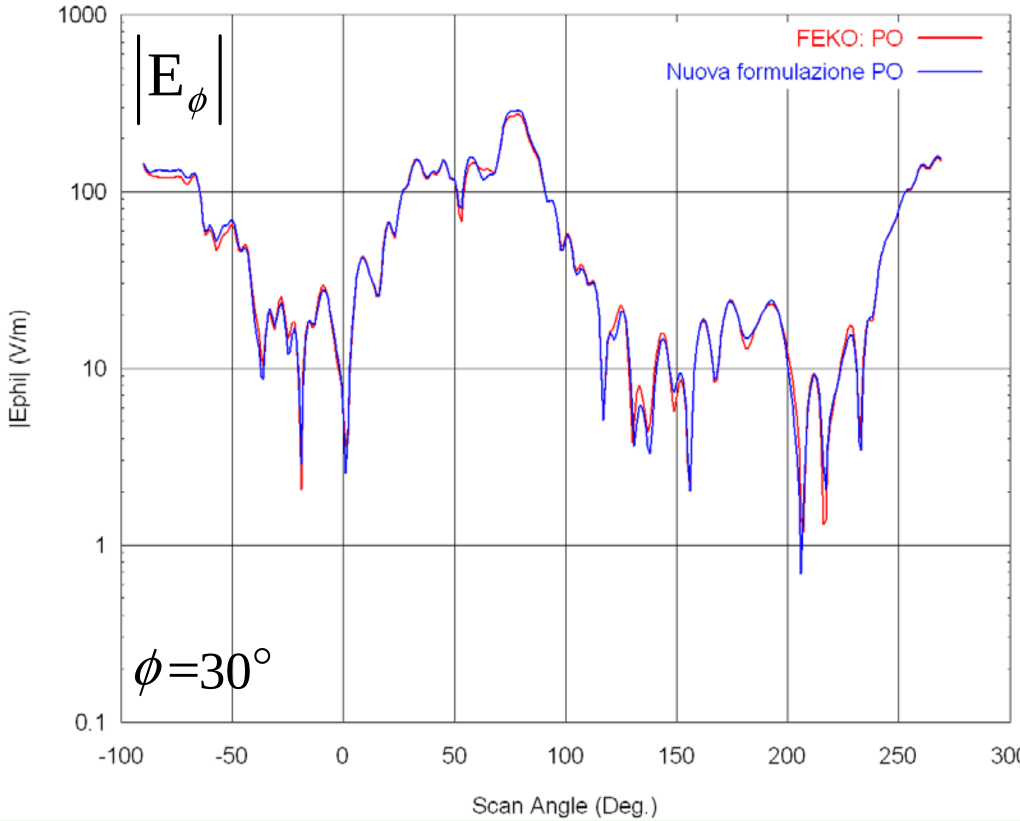

# NUMERICAL RESULTS

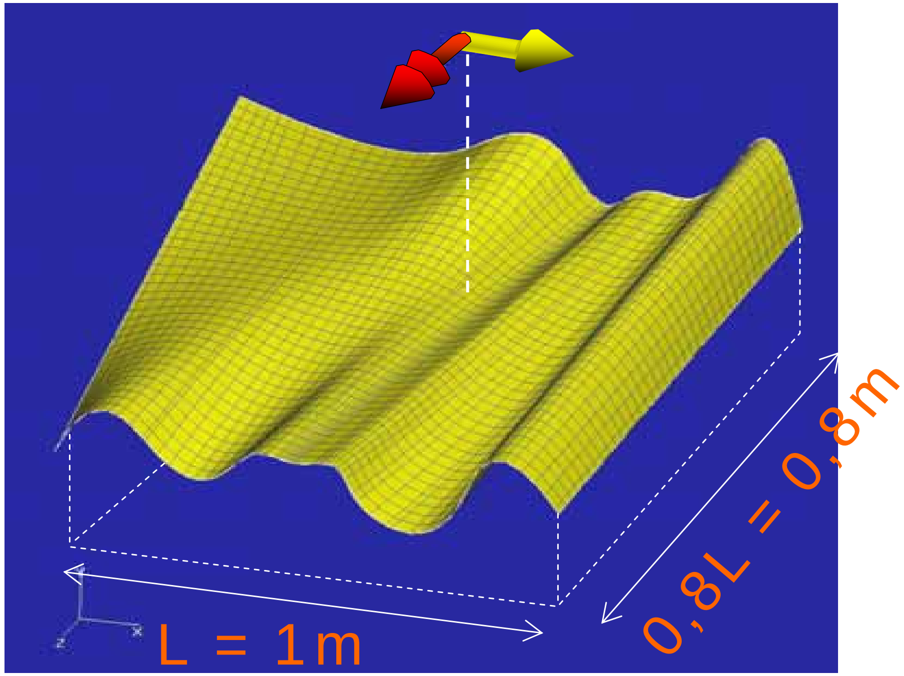


L ranging from 10λ  to 70λ

(3-21 GHz)

Max curvature radius:
ranging from 1,5λ to 8λ

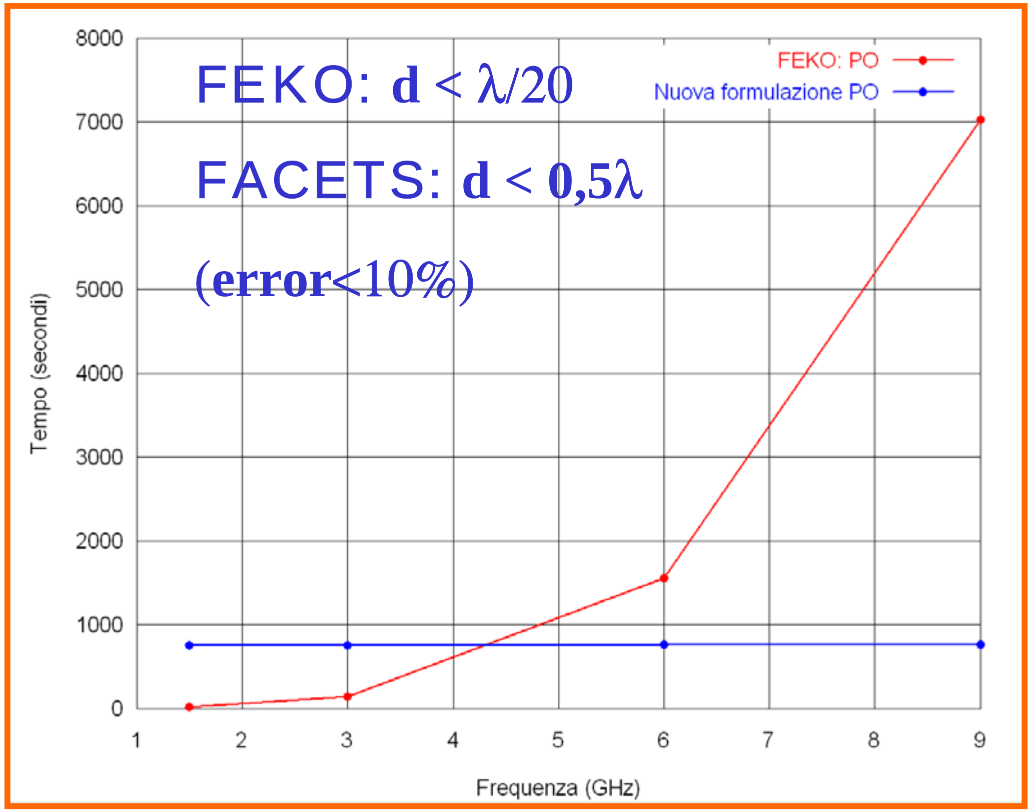

# EXTENSION TO CURVED REFLECTORS

- Let us consider an **arbitrarily curved p.e.c. surface**, illuminated by an hertzian dipole. By defining two auxiliary problems (pertaining the GO incident and reflected fields), the PO field can be represented by a pair of integrals over the GO equivalent currents on the two SB's.

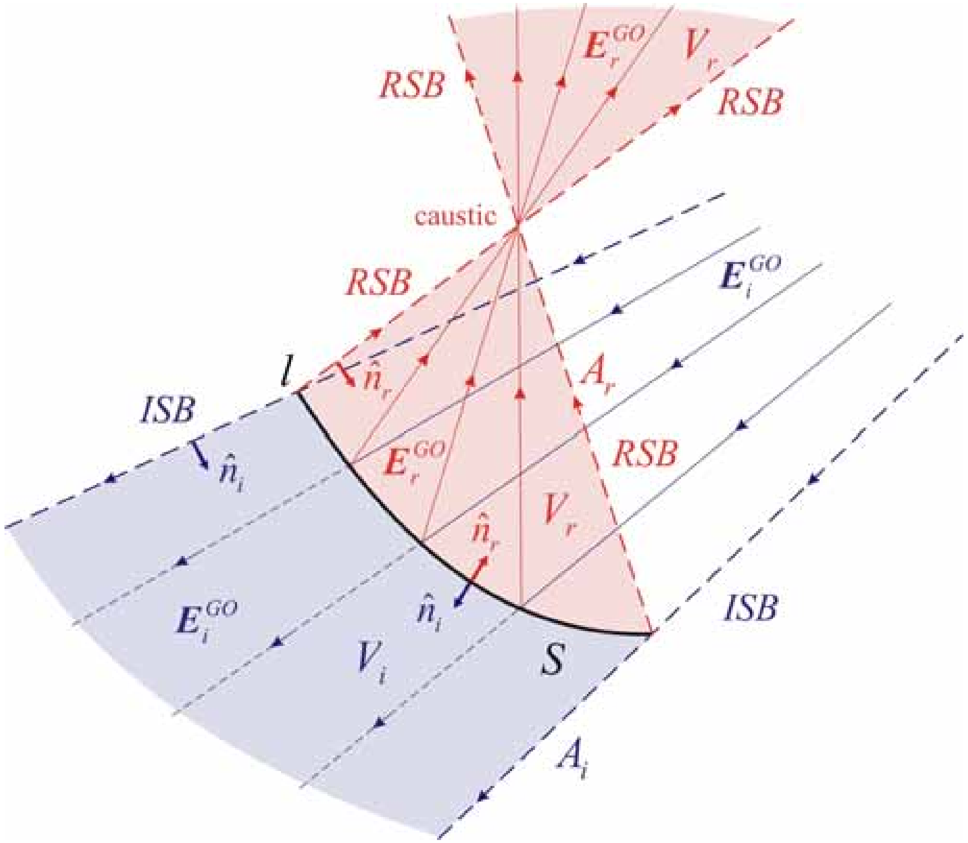


- The geometrical construct (→ equivalence principle applied to optical SB's) ensures

→ the GO equivalent currents are parallel to local incident or reflected ray direction

→ the GO equivalent currents exhibit a linear phase progression with the propagation wave-number of the surrounding medium

- The SBI treatment for surface-to-line integral reduction (→ exact evaluation of the elemental strip's radiation) can be carried out **only if**

→ the widening factor of the elemental strip on each of the SB's and the spreading factor of the relevant GO field exactly cancels each other

# FOCALLY-FED REFLECTORS

## Focusing properties

- The GO field reflected by a **hyperbolic or elliptic reflector**, which is fed from either of its focuses, can be thought of as originating from an image feed (**point-source**) at the other focus

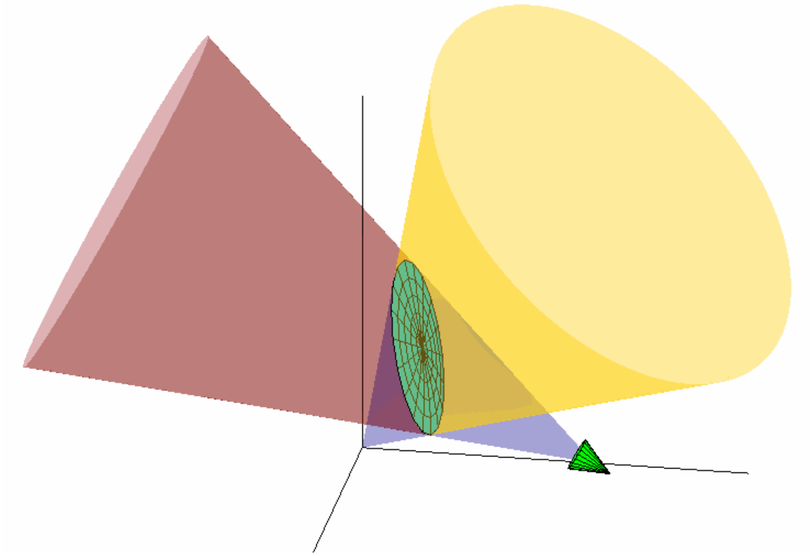

→ straightforward extension of the SBI formulation for flat surfaces

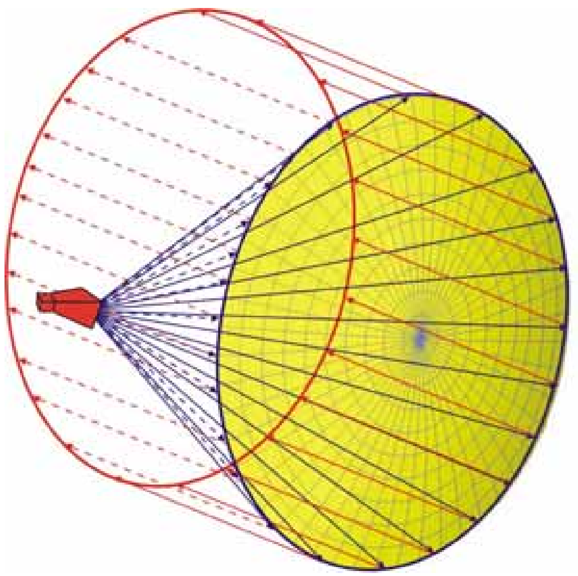

- The GO field reflected by a focally-fed **parabolic reflector** propagates along ray-paths which are all **parallel** to its axis (→ **plane wave-fronts**).

→ **not a plane wave** (non-uniform amplitude on a each plane wave-front)

- Parallel reflected rays → both widening and spreading factors are unity

→ exact evaluation of the radiation integral on an elemental strip of the RSB

# PARABOLIC REFLECTORS

- Offset configuration

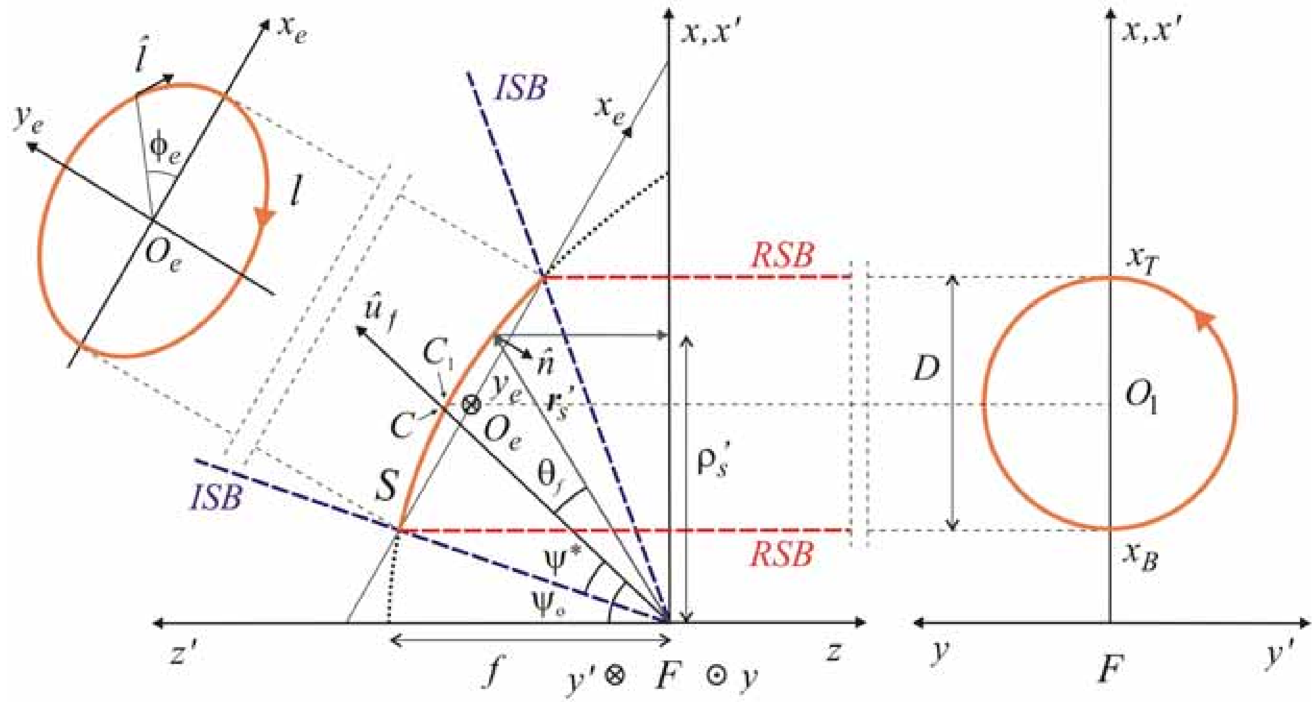


- Auxiliary problems

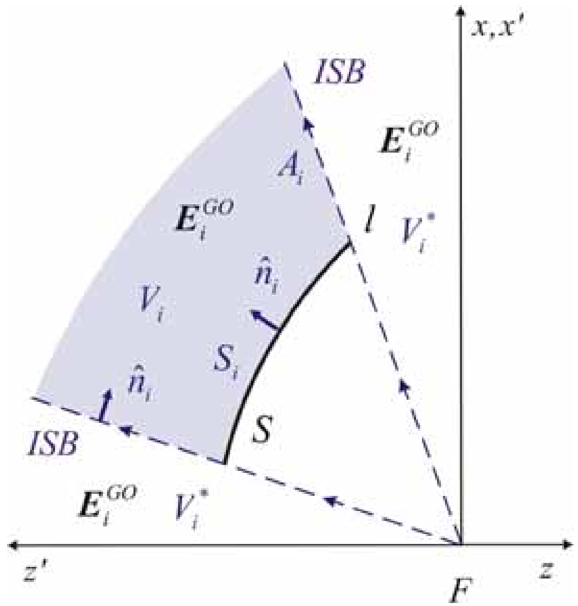


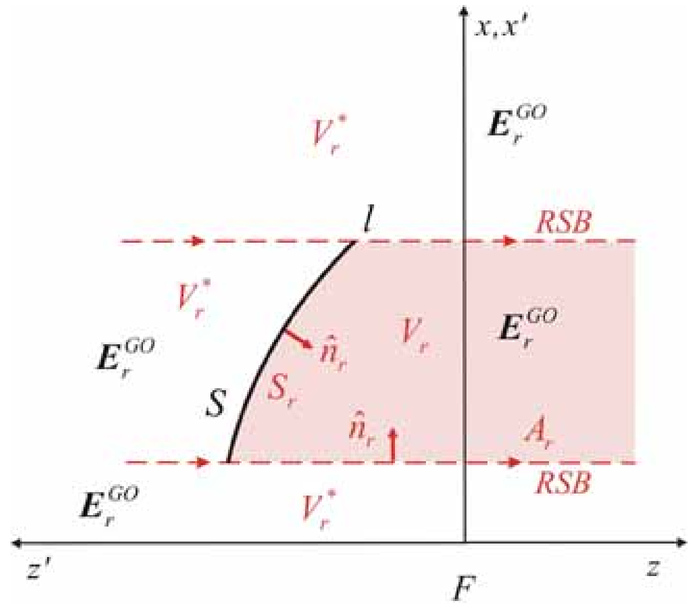

# CYLINDRICAL RSB

- The field contributions radiated by the equivalent currents on the **conical ISB** are described by the same expressions as those for a flat plate

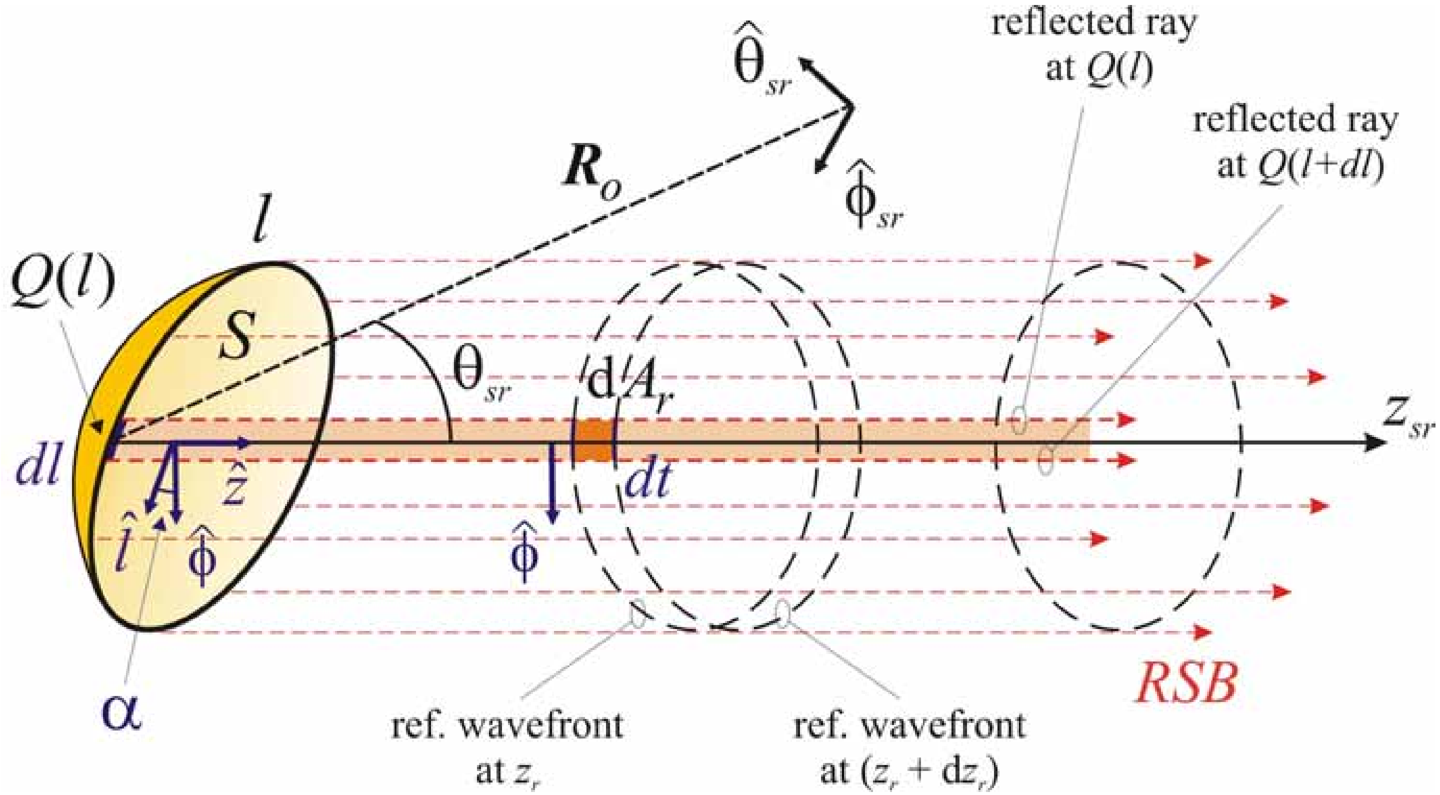


- The field contributions radiated by the equivalent currents on the **cylindrical RSB** are again described by the same expressions, but **the local spherical coordinate system at each point on the reflector's rim refers to a *z*-axis which is everywhere parallel to the reflector's axis**

# MAIN BEAM CAUSTIC

- The GO field of a focally-fed parabolic reflector exhibits a far-zone caustic in the main beam direction (→ along the reflector axis)

  → all the reflected rays point towards the same direction

  → the GO description fails there

- Under the far-zone limit, the RSB collapses in a single caustic direction

  → the incremental diffracted field radiated by each elemental strip is singular along the strip's direction itself

  → **all the incremental diffracted contributions from the edge of the parabolic reflector are concurrently singular in the main beam direction**

- In order to have a proper **far-field** compensation among all the singular contributions (and between the whole of them and the non-decaying GO field) a more accurate evaluation of diffraction phenomena would be required

  → accounts for further features of the field amplitude distribution (slope…)

- Due to this lack of compensation, the PO field predicted by the SBI formulation is affected in the far-zone region by some non-physical behavior at the main lobe caustic direction and close to this one.

# FROM NF TO FF

- No drawback occurs when observing from near to intermediate regions
  - → the RSB is composed of geometrically distinct ray-paths
  - → along each strip, only one incremental field is singular; all the other are well-behaved

- The SBI formulation for parabolic reflectors can be conveniently used to evaluate fields in the near field region (FFT algorithms cannot be applied)
  - → illumination of independent objects placed in the vicinity of the reflector (e.g. sub-reflectors, struts, etc.)

- In order to evaluate far-field pattern, a very effective and efficient approach is obtained by combining the SBI field estimates in intermediate region with a **FFT** of the far-field radiation integral over the corresponding equivalent currents
  - → similar to FFT of GO/AI (same efficiency)
  - → unlike the GO field, the SBI representation also accounts for diffraction (more accurate estimates of field's samples)

# NUMERICAL RESULTS

- Near-Field $E_x$ pattern at ***z = 1λ*** for different Gaussian feed edge illuminations

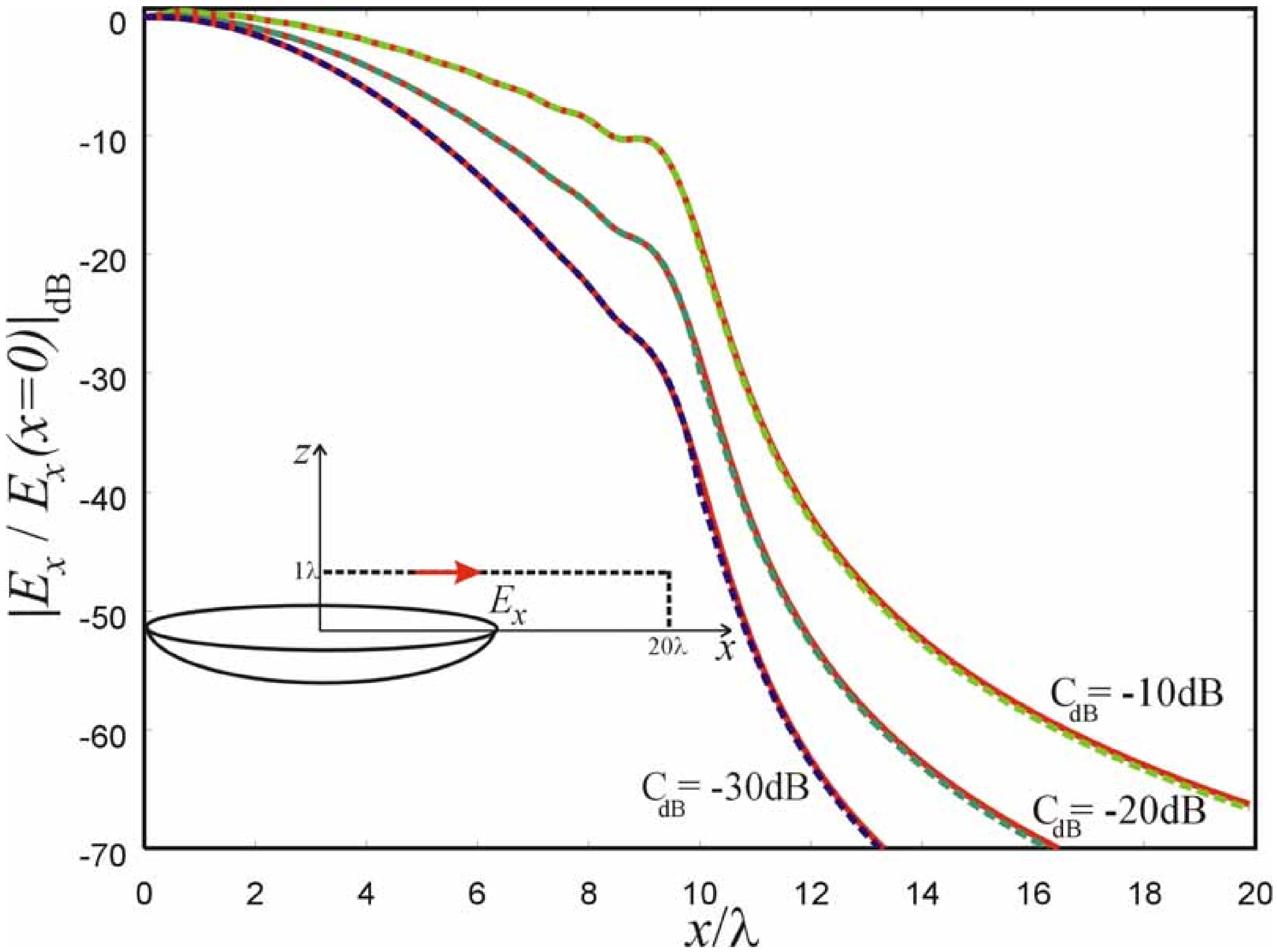


Surface Integration

Line Integration

**-10 dB**

**-20 dB**

**-30 dB**

# NUMERICAL RESULTS

- Near-Field $E_x$ pattern at ***z* = 5*λ*** for different Gaussian feed edge illuminations

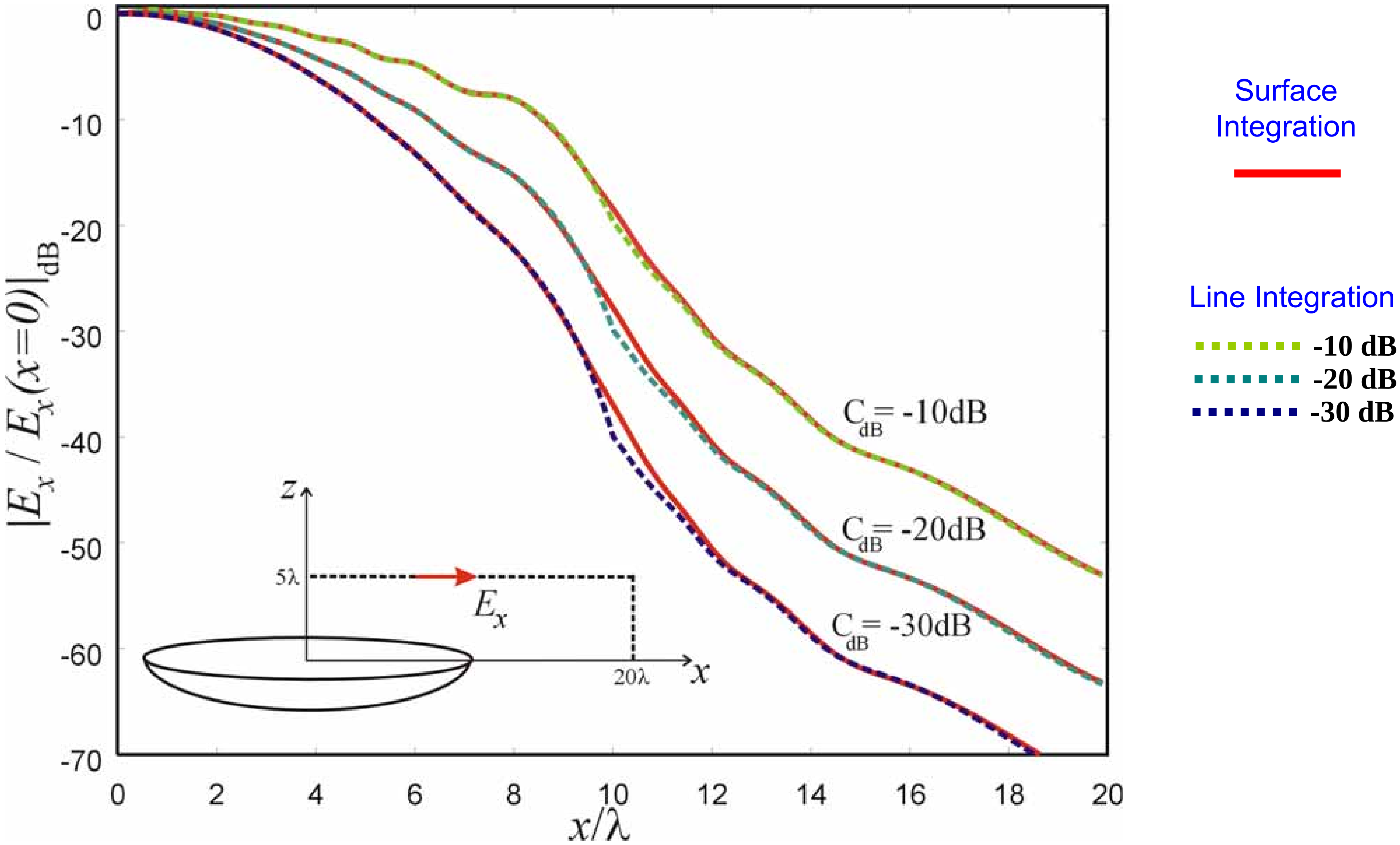

# HYPERBOLIC REFLECTORS

- Hyperbolic reflectors are widely used as subreflectors in Cassegrain antenna systems

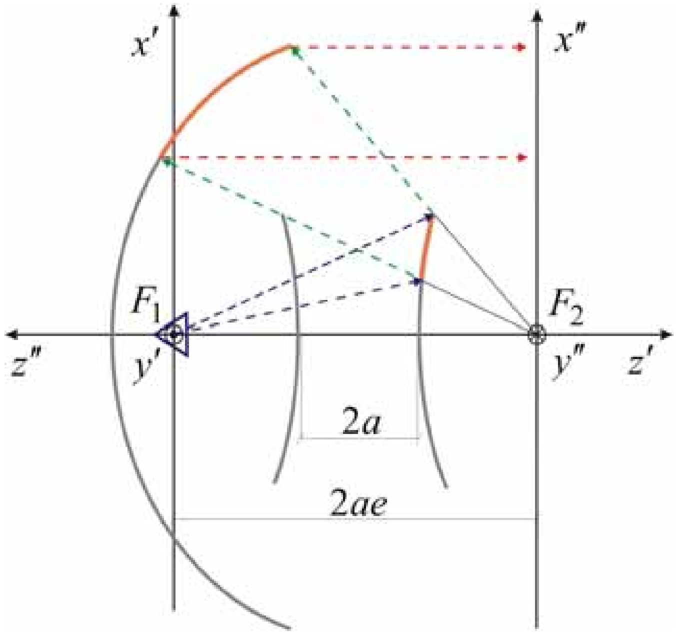


- In usual implementations of multi-reflector system (or of beam waveguides) all the elements are hyperbolic or elliptic reflectors (except the last, main parabolic dish)

- Auxiliary problems

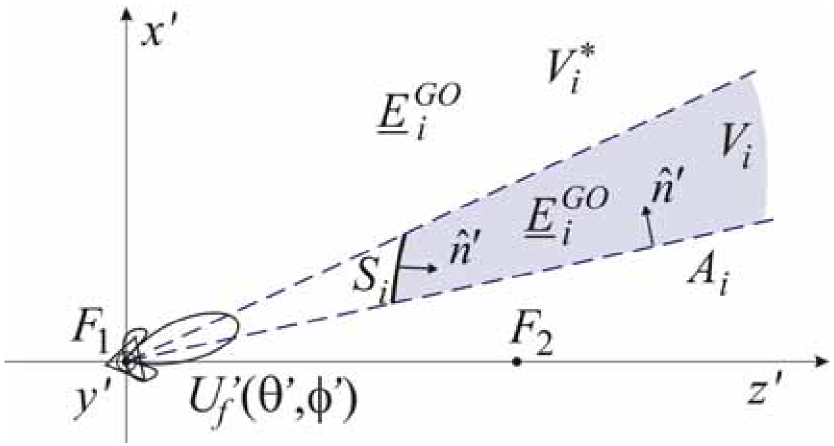


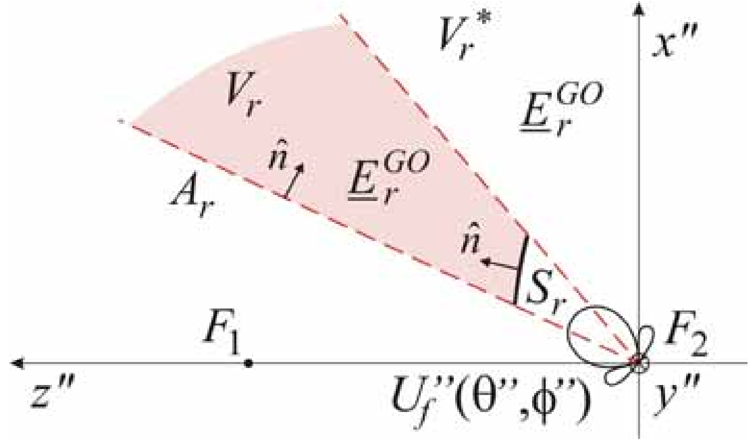


- The GO reflected field is that of an **image point-source**

→ the SBI representation for the PO field is exactly the same as that for flat plates (**same ray-system**)

# NUMERICAL RESULTS

- **Co-polar** component
- **Near region** of the reflector

- Offset angle, $\theta_0 = 50°$
- Half cone aperture, $\theta^* = 30°$

- Radial scan at fixed distance between the virtual focus and the observation point. The scan comprises the GO light region

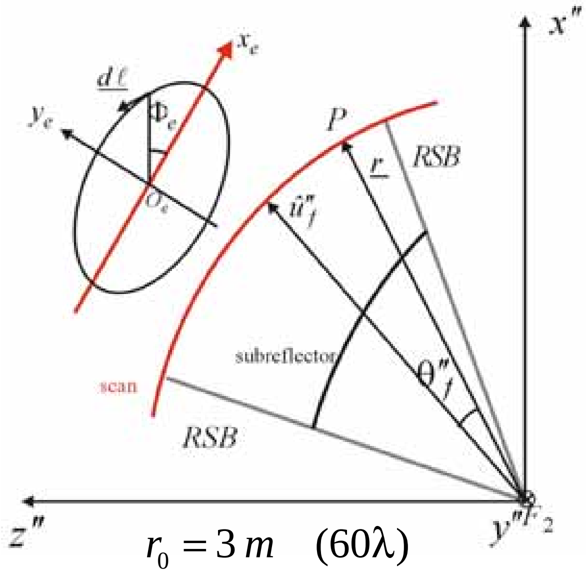


$$r_0 = 3\,m \quad (60\lambda)$$

$$\phi_e = 0 \quad (x'' - z''\ plane)$$

$$-1.5\,\theta^* < \theta''_f < 1.5\,\theta^*$$


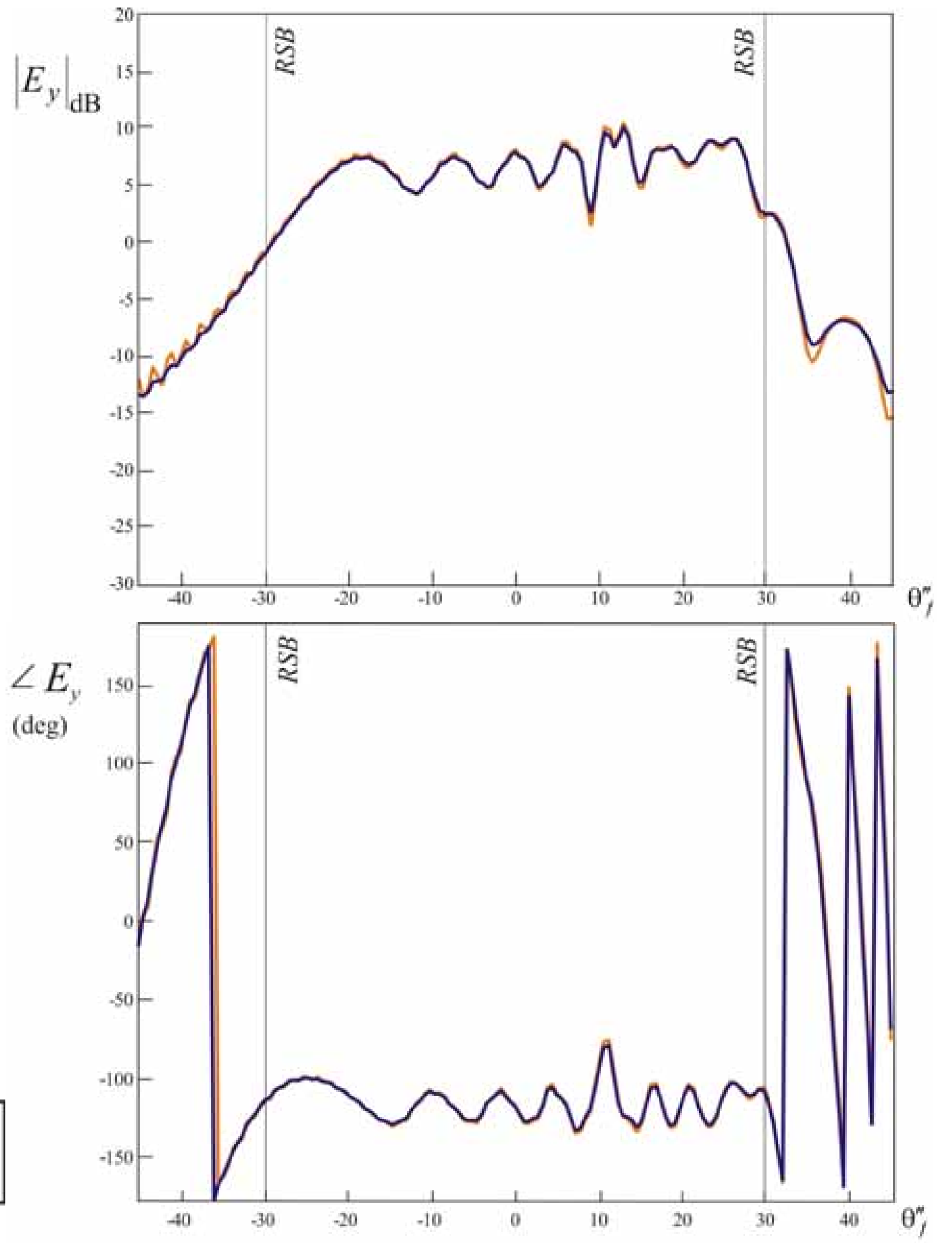

# NUMERICAL RESULTS

- **Cross-polar** component
- **Near region** of the reflector

- Offset angle, $\theta_0 = 50°$
- Half cone aperture, $\theta^* = 30°$

- Radial scan at fixed distance between the virtual focus and the observation point. The scan comprises the GO light region

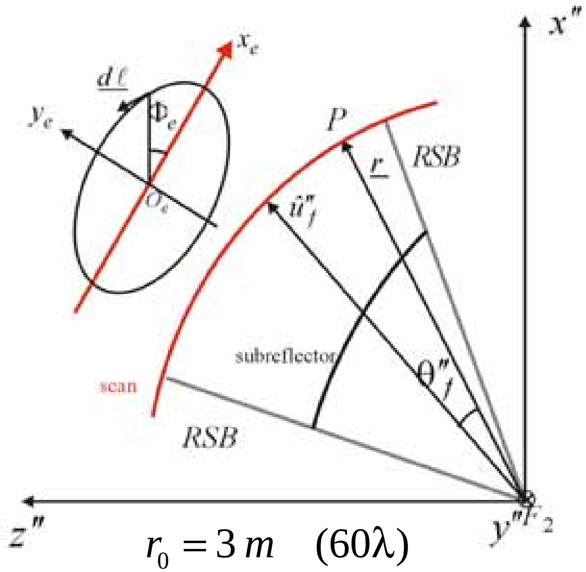


$$r_0 = 3\,m \quad (60\lambda)$$
$$\phi_e = 0 \quad (x'' - z''\ plane)$$
$$-1.5\,\theta^* < \theta''_f < 1.5\,\theta^*$$


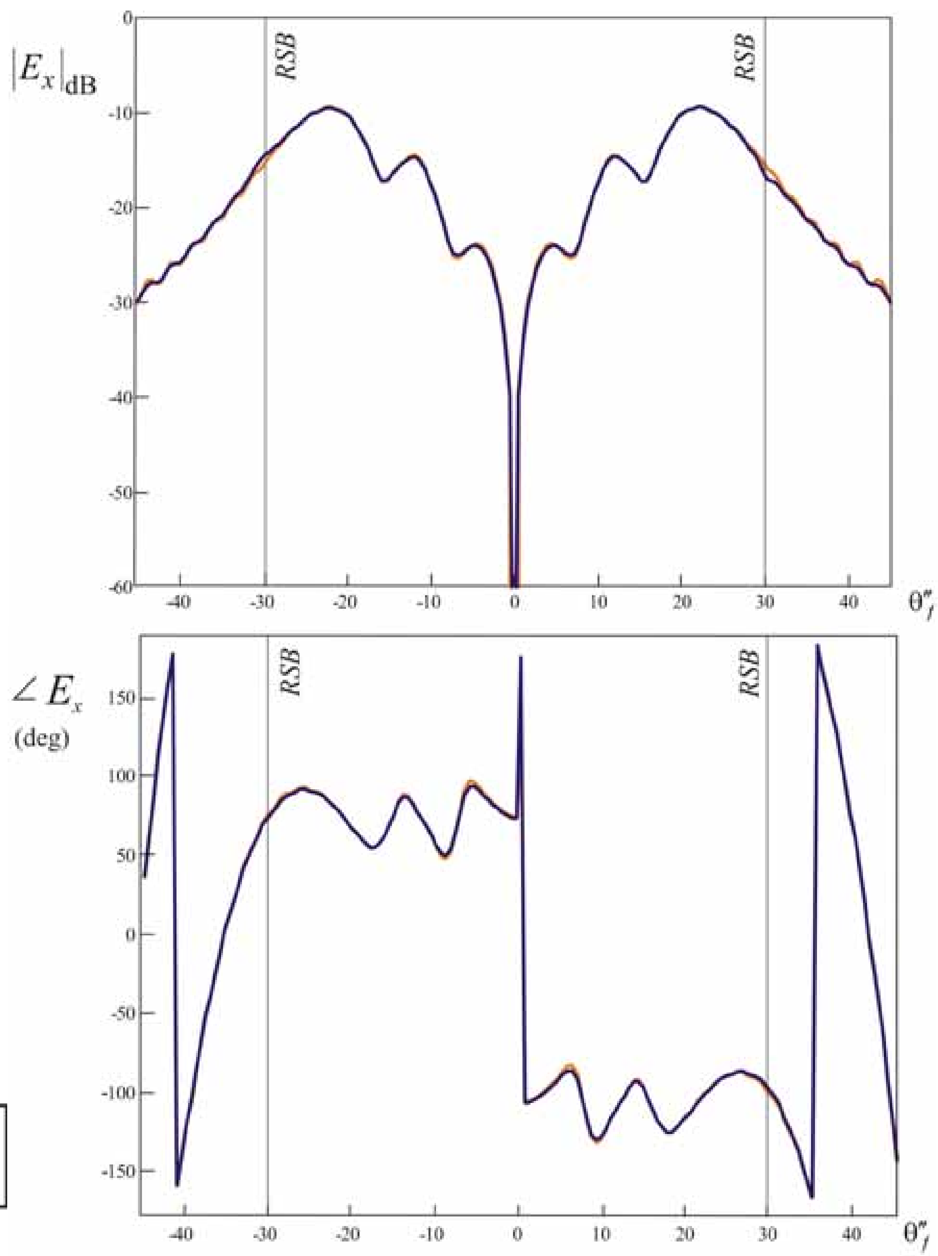

# NUMERICAL RESULTS

- $|\Delta E| / |E|_{max}$ **near field error**

cut at $\phi_e = 0$

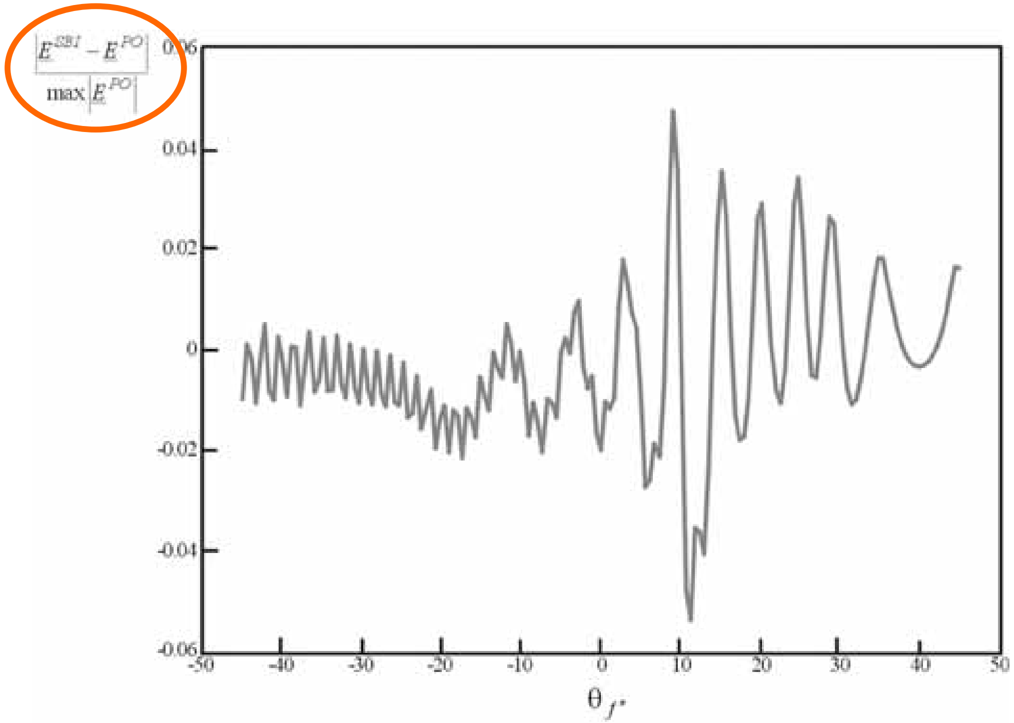


cut at $\phi_e = 90°$

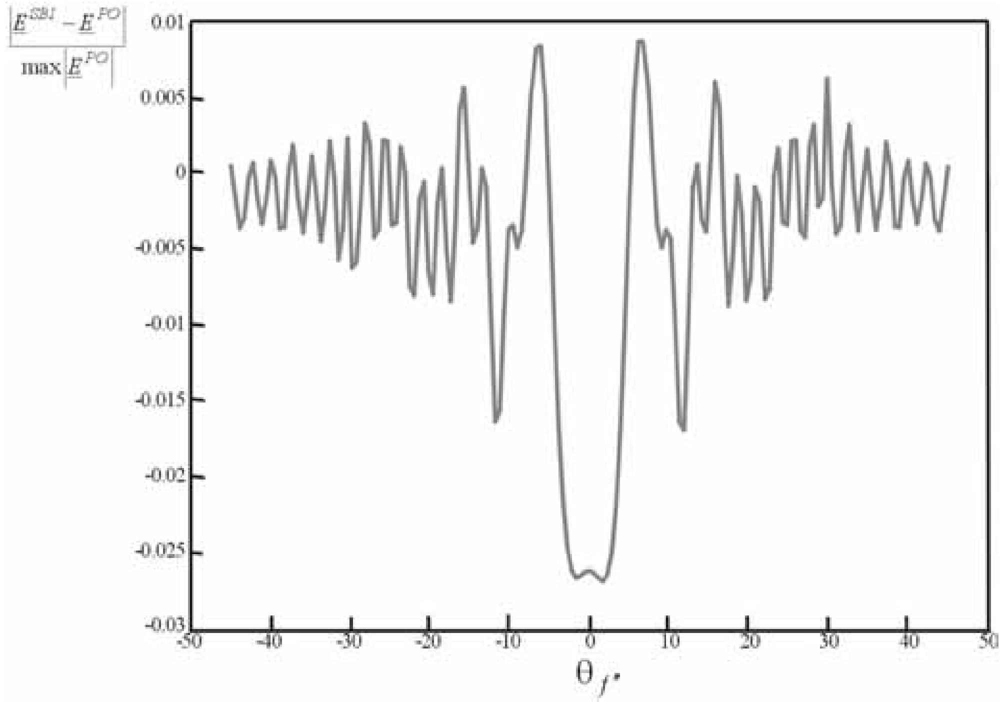

# COMPUTATIONAL COST COMPARISON

Speed improvement – hyper. reflector

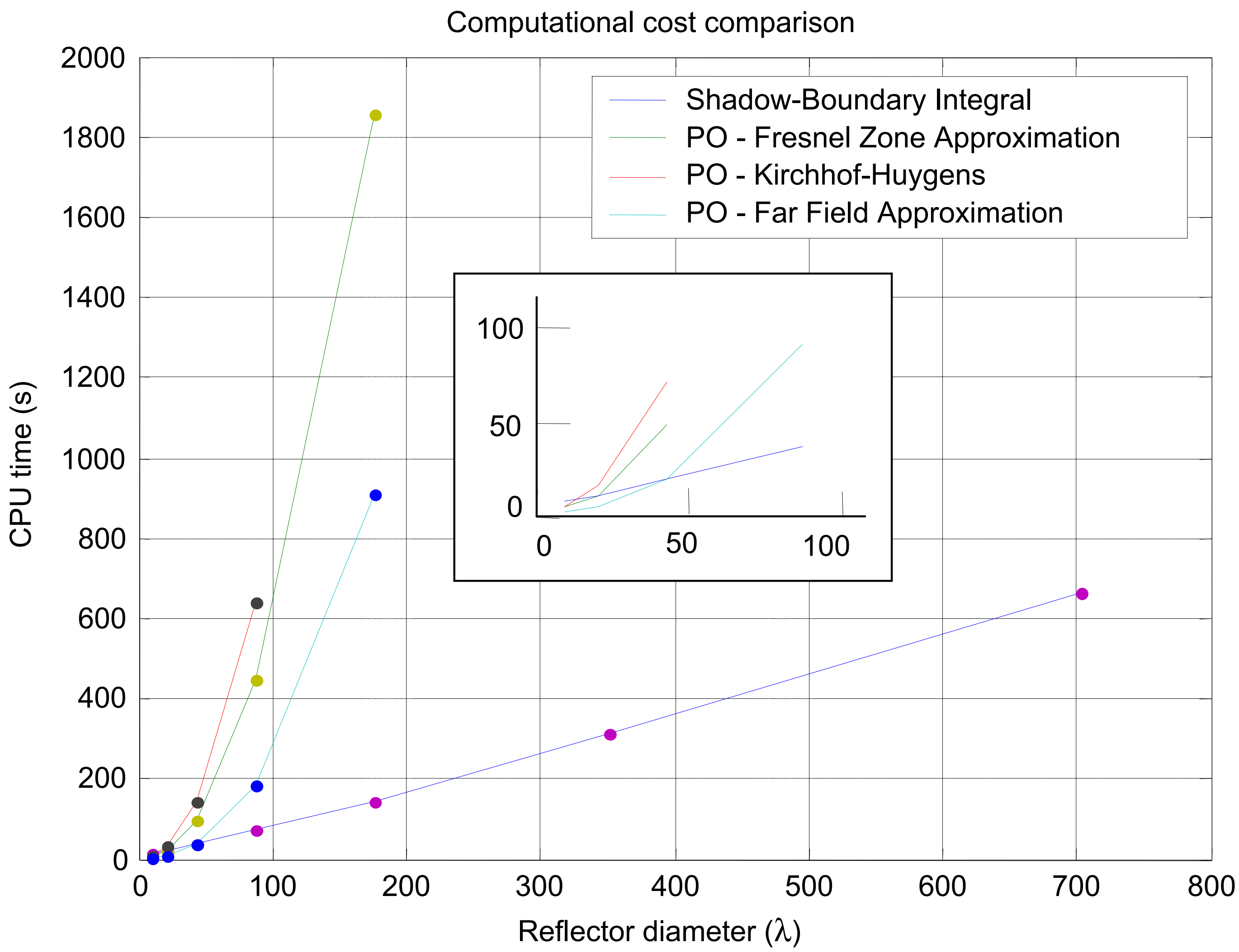


The dependence of CPU time on diameter of the antenna is linear

# COMPUTATIONAL COST EXTRAPOLATION

Speed improvement – hyper. reflector

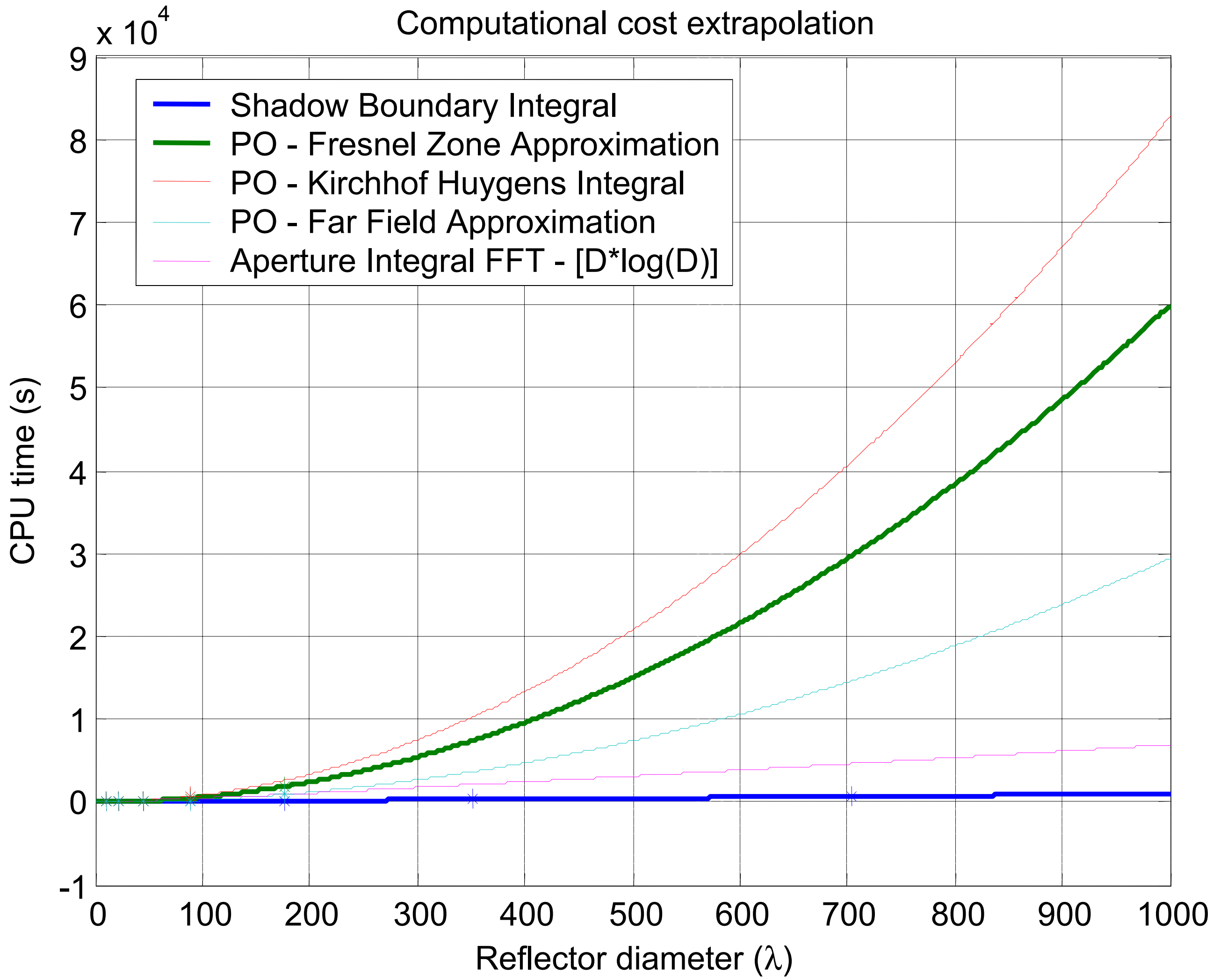


The dependence of CPU time on diameter of the antenna is linear

# ITD FRINGE AUGMENTATION

- Despite of the geometry of the scattering surface, the SBI formulation is well-suited to be improved by fringe diffraction contributions in the framework of edge-wave theories such as ITD

- Both the **SBI** and the **ITD** representations of the **diffracted field** consist of **distributed incremental contribution**, numerically integrated along the edge of the actual object

$$\boxed{\boldsymbol{E} = \boldsymbol{E}^{SBI} + \boldsymbol{E}^{f}} \longrightarrow \boxed{\boldsymbol{E}^{f} = \int_{\ell} \boldsymbol{e}^{f}(\ell)\, d\ell}$$

- This augmentation is expected to provide a significantly improved accuracy, when the aspect of observation deviates from those of GO reflection and incidence SBs, especially for cross-polar components.

# ITD FRINGE CONTRIBUTION

$$\boxed{\boldsymbol{e}^{f}(\ell)=\frac{e^{-jkr}}{2\pi r}\underline{\underline{D}}^{f}(\beta,\beta',\phi,\phi')\cdot\boldsymbol{E}_{i}^{GO}(\ell)}$$

$$\underline{\underline{D}}^{f}=D_{11}^{f}\,\hat{\beta}\hat{\beta}'+D_{12}^{f}\,\hat{\beta}\hat{\phi}'+D_{22}^{f}\,\hat{\phi}\hat{\phi}'$$

$$D_{11}^{f}(\beta,\beta',\phi,\phi')=d_{2}^{f}(\beta,\beta',\phi-\phi')-d_{2}^{f}(\beta,\beta',\phi+\phi')$$

$$D_{22}^{f}(\beta,\beta',\phi,\phi')=d_{2}^{f}(\beta,\beta',\phi-\phi')+d_{2}^{f}(\beta,\beta',\phi+\phi')$$

$$D_{12}^{f}(\beta,\beta',\phi,\phi')=-\mathrm{sgn}(z_{\ell}+z_{\ell}')\sqrt{1-\sin\beta\sin\beta'}$$

$$d_{2}^{f}(\beta,\beta',\Phi)=\frac{1}{2}\frac{\sqrt{\sin\beta\sin\beta'}\cos\frac{\Phi}{2}}{\sin\frac{\beta+\beta'}{2}+\sqrt{\sin\beta\sin\beta'}\sin\frac{\Phi}{2}}$$

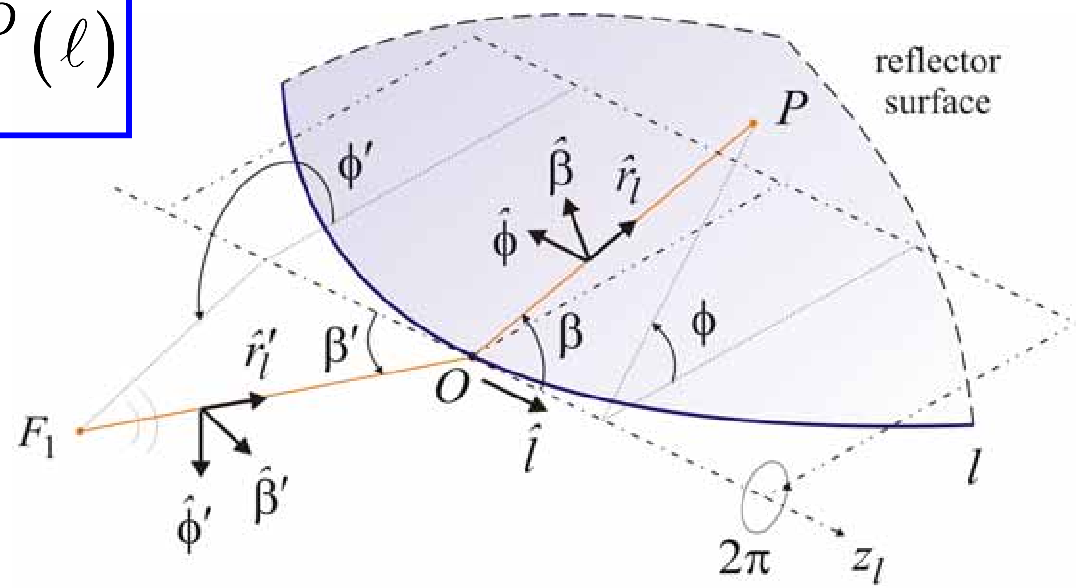


As usual in diffraction problems, the diffraction coefficients are formulated w.r.t. a different, local spherical $(r,\beta,\phi)$ reference system, with its origin at any point $O$ on the rim

- The ITD fringe diffraction coefficients are determined by subtracting the incremental contribution deduced from the PO field canonical problem, from that relevant to the total diffracted field.

# TEST CASE

- non-offset ($\theta_0$ = 0°; $\theta^*$ ≈ 71°; $e$ ≈ 1.45) hyperbolic reflector – vertical electric hertzian dipole in the primary focus

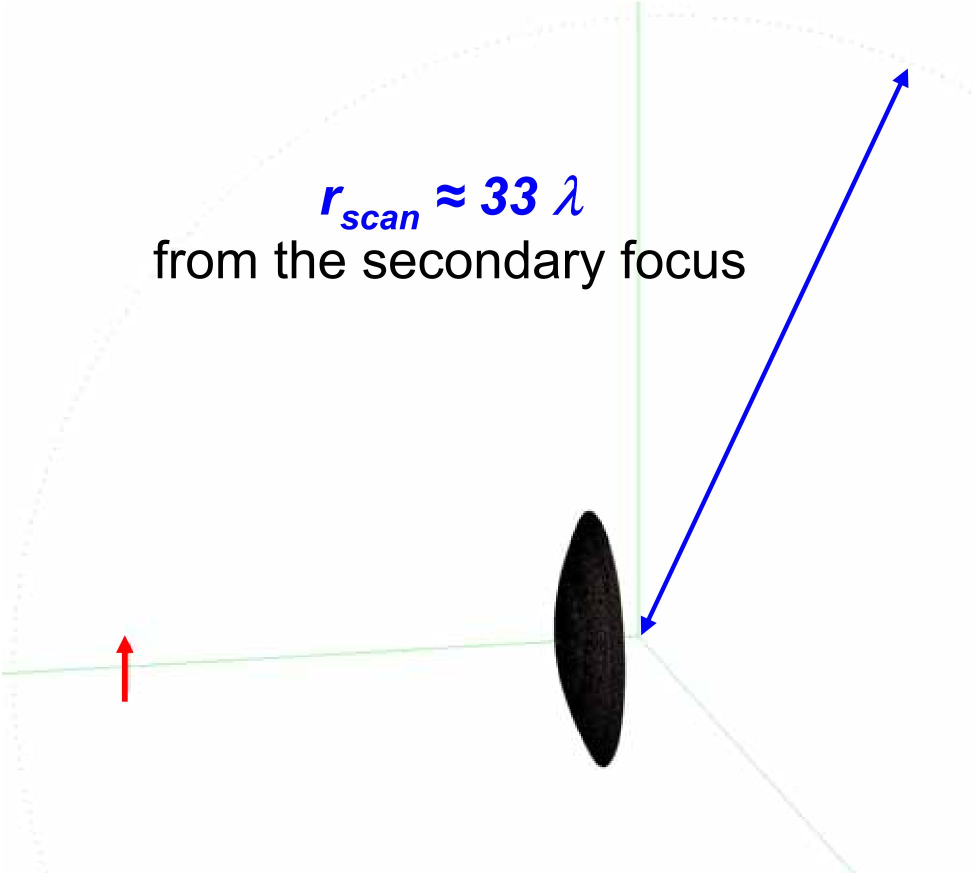



**SBI + ITD vs. MoM** (Feko™)

# NUMERICAL RESULTS

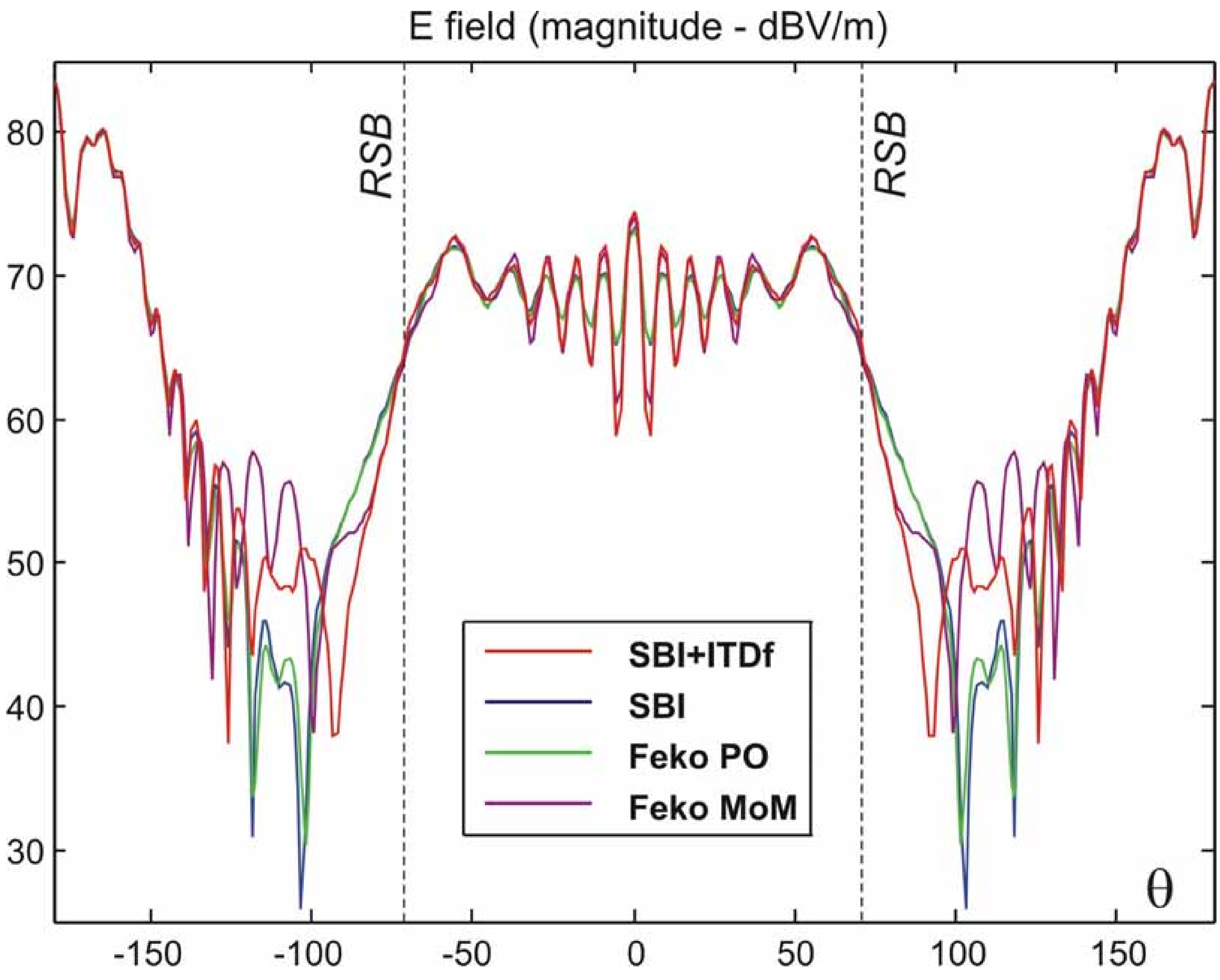


CPU times

| | |
|---|---|
| SBI+ITDf | 28.8 s |
| MoM | 1 h 19 m 3 s |

# APPLICATION TO A CASSEGRAIN ANTENNA

- The proposed SBI method has been implemented with a model of the complete Cassegrain system (hyperbolic sub & parabolic main reflector).
- In order to maintain a field representation that requires only one line integration per reflector, the double interactions between the two reflectors have been accounted for as follows

| interaction | sub | main |
|---|---|---|
| **R - R** | GO (image source) | GO (“plane wave”) |
| **R - D** | GO (image source) | SBI + $ITD_{fringe}$ |
| **D - R** | SBI + $ITD_{fringe}$ | GO (ray tracing) |
| **D - D** | SBI + $ITD_{fringe}$ | ITD |

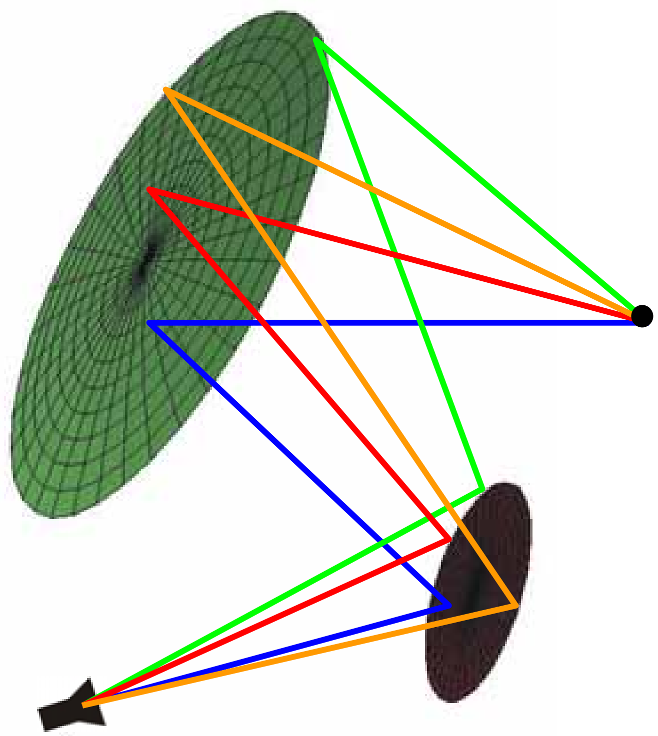

# CONCLUDING REMARKS

- The SBI shows a linear dependence of the computational cost on reflector size and significantly accelerates the field calculation for large reflector antenna.
- Accuracy is very good (comparable to PO), for both co-polar and cross-polar components (amplitude and phase) .
- An ITD fringe augmentation can provide an even improved accuracy, without compromising the computational efficiency.
- The SBI-ITD formulation can be applied to evaluate the field radiated by a complete Cassegrain antenna system by means of a double line integration (vs the “classical” double surface integration).
- Further work & possible extensions:
  - include modelling of out-of-focus source;
  - extend SBI to non-canonical surfaces.